Recovery of hydrothermal vent communities in response to an induced disturbance at the Lucky Strike vent field (Mid-Atlantic Ridge)

J. Marticorena, M. Matabos, E. Ramirez-Llodra, C. Cathalot, A. Laes-Huon, R. Leroux, Stephane Hourdez, J.-P. Donval, J. Sarrazin

Graphical Abstract

Vent communities of
Bathymodiolus azoricus
Lucky Strike vent field
MAR, 1700 m

Experimental disturbance by removing faunal assemblages

10 cm

10 cm
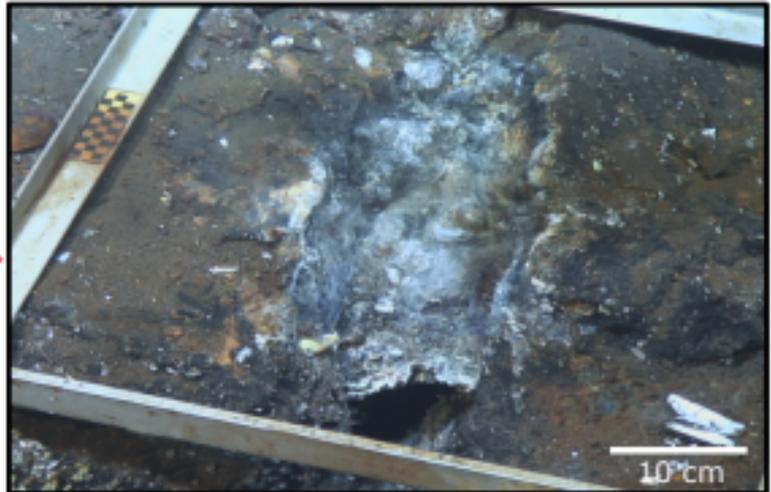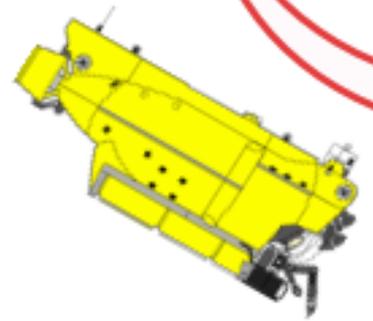
High recovery in taxonomic richness
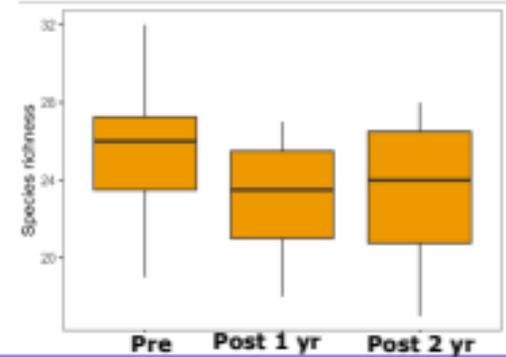
Incomplete recovery in faunal density

Pre   Post 1 yr   Post 2 yr

Pre   Post 1 yr   Post 2 yr
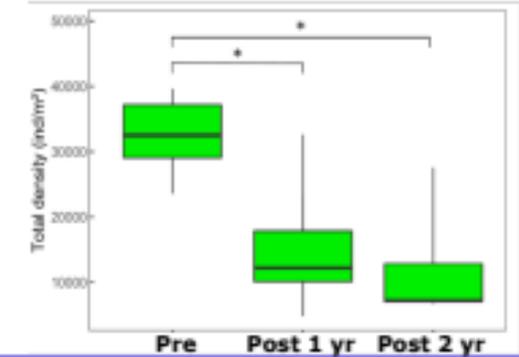
Assess the recovery and follow the recolonisation process within 2 years
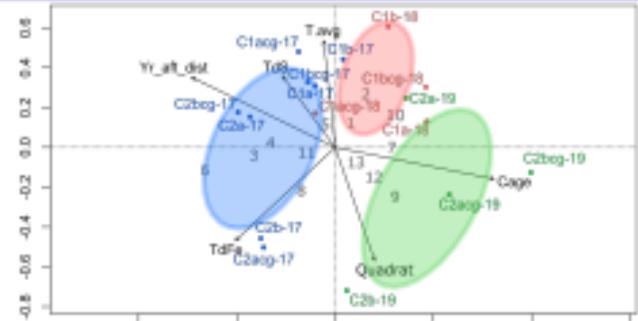
Significant difference in faunal composition in pre-disturbed, 1 and 2 years after disturbance
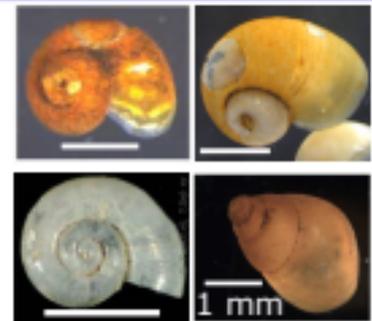
Gastropod species pioneer colonists

1 mm

Recovery of hydrothermal vent communities in response to an induced disturbance at the Lucky Strike vent field (Mid-Atlantic Ridge)

Marticorena J.[1]*, Matabos M.[1]*, Ramirez-Llodra E.[2,3], Cathalot, C.[4], Laes-Huon, A.[5], Leroux R.[6], Hourdez S.[7], Donval J-P.[4], Sarrazin J.[1]*

[1] *Ifremer, REM/EEP, F-29280 Plouzané, France*

[2] *Norwegian Institute for Water Research, Gaustadalleen 21, 0349 Oslo, Norway*

[3]*REV Ocean, Oksenøyveien 10, 1366 Lysaker, Norway*

[4] *Ifremer, REM/GM/LCG, F-29280 Plouzané, France*

[5] *Ifremer, REM/RDT/LDCM, F-29280 Plouzané, France*

[6] *Research Centre for Watershed-Aquatic Ecosystem Interactions, Université du Québec à Trois-Rivières, Trois-Rivières, QC G9A 5H7, Canada*

[7] *Observatoire Océanologique de Banyuls-sur-Mer, UMR 8222 CNRS-SU, 1 avenue Pierre Fabre, 66650, Banyuls-sur-Mer, France.*

*Corresponding authors : Julien Marticorena (julienmarticorena@gmail.fr), Marjolaine Matabos (Marjolaine.matabos@ifremer.fr), Jozée Sarrazin (Jozee.sarrazin@ifremer.fr),

Abstract

So far, the natural recovery of vent communities at large scales has only been evaluated at fast spreading centres, by monitoring faunal recolonisation after volcanic eruptions. However, at slow spreading ridges, opportunities to observe natural disturbances are rare, the overall hydrothermal system being more stable. In this study, we implemented a novel experimental approach by inducing a small-scale disturbance to assess the recovery potential of vent communities along the slow-spreading northern Mid-Atlantic Ridge (nMAR). We followed the recovery patterns of thirteen Bathymodiolus azoricus mussel assemblages colonising an active vent edifice at the Lucky Strike vent field, in relation to environmental conditions and assessed the role of biotic interactions in recolonisation dynamics. Within 2 years after the disturbance, almost all taxonomic richness had recovered, with the exception of a few low occurrence species. However, we observed only a partial recovery of faunal densities and a major change in faunal composition characterised by an increase in abundance of gastropod species, which are hypothesised to be the pioneer colonists of these habitats. Although not significant, our results suggest a potential role of mobile predators in early-colonisation stages. A model of post-disturbance succession for nMAR vent communities from habitat opening to climax assemblages is proposed, also highlighting numerous knowledge gaps. This type of experimental approach, combined with dispersal and connectivity analyses, will contribute to fully assess the resilience of active vent communities after a major disturbance, especially along slow spreading centres targeted for seafloor massive sulphide extraction.

1. Introduction

Deep-sea hydrothermal vents are mainly distributed along mid-ocean ridges and back-arc basins. Vent communities are considered as productivity hotspots with a high level of endemic fauna (Tunnicliffe, 1991) that thrives mainly on chemoautotrophic primary production (Childress and Fisher, 1992). Faunal assemblages are often dominated by symbiotic foundation species such as siboglinid tubeworms, mytilid mussels, large provannid gastropods or alvinocaridid shrimps, which promote local diversity by providing 3D structures and enhancing habitat heterogeneity (Dreyer et al., 2005; Govenar and Fisher, 2007). At the edifice scale, faunal distribution consists in a mosaic of assemblages mainly influenced by environmental conditions and patchiness of fluid emissions (Sarrazin et al., 1997; Sarrazin and Juniper, 1999; Luther et al., 2001; Gollner et al., 2010; Marsh et al., 2012; Husson et al. 2017). Indeed, species colonise the mixing gradient depending on their physiological tolerance to environmental conditions, nutritional requirements and biotic interactions (e.g. predation, facilitation; Levesque et al. 2003, Mullineaux et al. 2003, Sancho et al. 2005). Biotic interactions were suggested to prevail in high diffuse-flow areas where the resources are not limited, while facilitation will predominate in habitats with lower fluid input (Mullineaux et al. 2003). As observed in coastal hard substrate communities, mosaics are highly dynamic and patche's size and boundaries amongst the patched may change through time (Connell and Keough, 1985). At large spatial scale, the patchiness of vent habitat results in a network of metacommunities and population connectivity is insured by dispersal of planktonic larvae (Mullineaux et al., 2018).

Hydrothermal vents are naturally subject to stochastic major disturbance such as volcanic eruptions that may eradicate faunal assemblages at the vent-field scale. On the other hand, since the first discovery of hydrothermal vents and associated seafloor massive sulphide (SMS) deposits, more than 40 years ago, the interest of mining companies for commercial exploitation of their high metal content has been increasing (Corliss et al., 1979; Spiess et al., 1980; Van Dover, 2011). These industrial activitiy has not yet started, but it is predicted that they may induce different levels of impacts (Boschen et al., 2013; Cuvelier et al., 2018; Orcutt et al., 2020), including physical destruction of habitats and the complete eradication of their faunal communities within the mining site (Van Dover 2007). The creation of a sediment plume may also affect different biological processes, such as reproduction, dispersal, mobility

and feeding strategies at larger scale (Van Dover, 2010; Boschen et al., 2013; Gollner et al., 2017; Suzuki et al., 2018; Washburn et al., 2019). However, there are still many uncertainties about community resilience, and the time-scale needed for a possible recovery of the impacted ecosystems (Cuvelier et al., 2018).

Disturbance in mosaic habitats such as active vents may play an important role in initiating, maintaining or enlarging patches within established assemblages (Sousa 1985; Denny 1987). The fundamental question of recolonisation and recovery of vent assemblages after a disturbance can be studied in a metacommunity framework, using a patch dynamics approach in which the colonisation and persistence of impacted area is highly dependent on dispersal across vent fields and local disturbance regimes (Leibold et al., 2004; Mullineaux et al., 2018). At local scale, the settlement of post-larvae is influenced by environmental conditions and habitat suitability and recolonisation dynamics are also dependent on biotic interactions that may induce facilitation or competitive exclusion (Mullineaux et al., 2003; Sancho et al., 2005). Understanding processes acting at small scales are paramount in evaluating mechanisms controlling successional dynamics after recolonisation by species from afar.

At active vents, the few examples of recovery are based on studies linked to large-scale natural disturbances caused by volcanic and tectonic activities (Butterfield et al., 1997; Tunnicliffe et al., 1997; Shank et al., 1998; Marcus et al., 2009; Gollner et al., 2015a). The frequency of such disturbances is highly variable among vent systems, depending on their geological settings. At fast-spreading ridges, where vent sites are separated by a few kilometers, volcanic eruptions occurs with time intervals of a decade (Tolstoy et al. 2006) and macrofaunal communities show a fairly good recovery of diversity and densities within few years following the various eruptions (Tunnicliffe et al. 1997; Shank et al. 1998; Marcus et al. 2009; Gollner et al. 2015a, 2017, 2020). However, differences in the sampling methodology between these studies (e.g. some used visual surveys while others sampled faunal assemblages) and the faunal compartment considered lead to differences in the estimation of recovery rates. Moreover, little information about the pre-disturbed baseline communities was available, making the comparison with post-disturbance communities difficult. Differences in community composition after re-colonisation were also observed (Mullineaux et al., 2020, 2012) and the prolonged monitoring of diversity showed that community composition was still changing ten years after the disturbance, suggesting that the disturbed

assemblages did not reach a climax stage during this time period (Mullineaux et al., 2020). Conversely, at slow spreading ridges, vent sites are separated by hundreds of kilometers (Beaulieu et al., 2015) and opportunities to observe natural disturbances are rare. Therefore, assessing the recovery ability of communities requires the use of alternative indirect approaches. One way is to use population connectivity data to estimate the recolonisation potential of key species, and thus infer vent community recovery rates (Baco et al., 2016; Breusing et al., 2016) as it was done by Suzuki et al. (2018). Their dispersal network analysis on species from 131 vent fields of the western Pacific Ocean estimated that a full recovery to original communities would take from 6 to 130 years. The slow recovery rate estimated in comparison to fast-spreading centers may notably be due in part to differences in topography that may reduce horizontal dispersal and connectivity (Mullineaux et al. 2018). However, this approach based on dispersal ability does not take into account the local factors influencing faunal establishment and many uncertainties remain regarding the role of biotic and abiotic conditions in recolonisation dynamics and ecological succession once the larvae reach the disturbed area.

In the present study, we provide an early evaluation of the recovery potential of active vent communities to a small-scale (< 1 m²) disturbance experiment initiated in 2017 on the Lucky Strike (LS) vent field, northern Mid-Atlantic Ridge (nMAR). After removing the fauna, we followed during 2 years the recolonisation dynamics of *Bathymodiolus azoricus* mussel assemblages and their habitats on a series of experimental quadrats. This experimental setting allowed us to describe the pre-disturbed structure of vent communities on the Montségur edifice (LS) and to monitor the recolonisation of benthic communities after the disturbance. The main objective of this work is to identify the role of biotic and abiotic conditions on recolonisation dynamics at the edifice scale, through the use of cages and measurements of environmental conditions. We expected that microbial communities would first colonise the bare substratum, followed by grazers (including several species of gastropods) that may feed on microbial mats. The engineer species *B. azoricus* would take more time to fully occupy the space, its presence facilitating the establishment of associated taxa and contributing to increasing diversity. We anticipated that mobile predators (e.g. shrimps, crabs or fishes) would play a major role in patch colonisation, influencing the first step of recovery. Although the scale and target of this experiment strongly differ from large-scale disturbance, our results

139 provide fundamental knowledge on recolonisation patterns of active hydrothermal vent

140 habitats at the edifice scale.

2. Material and methods

141

142

2.1. Study site

144 The Lucky Strike (LS) vent field is a basalt-hosted vent field situated close to the Azores Triple

145 Junction on the northern part of the Mid Atlantic Ridge (MAR) (Langmuir et al., 1997) (Fig. 1A).

146 LS contains over twenty active hydrothermal edifices distributed around a circular fossilised

147 lava lake at an average depth of 1700 m (Ondreas et al., 2009). Montségur is a small active

148 sulphide edifice that extends over a surface of 24 m x 16 m. It is located on a flat hydrothermal

149 slab at the south-east of LS (Fig. 1B). At least seven black smokers have been identified on the

150 edifice, in addition to the extensive diffuse low-temperature discharges through cracks at its

151 base and on its flanks (Barreyre et al., 2014). Montségur is covered by dense mussel

152 assemblages of the engineer species *Bathymodiolus azoricus*. Vent faunal communities

153 inhabiting diffuse flow areas on and around the edifice are characterised by high-density

154 populations of gastropods (*Protolira valvatoides, Lepetodrilus atlanticus, Pseudorimula*

155 *midatlantica*), polychaetes (*Branchipolynoe seepensis, Amphisamytha lutzi*) and shrimps

156 (*Mirocaris fortunata*) (Sarrazin et al. 2020)*.*

2.2. Experimental setup

158 In July 2017, an experimental setup was deployed during the Momarsat cruise on board the

159 R/V "*Pourquoi pas ?*" using the Remotely Operated Vehicle (ROV) *Victor6000*. Thirteen

160 stainless steel quadrats (50 x 50 cm), equipped with pyramidal structures on top, were

161 installed over *Bathymodiolus azoricus* assemblages (Fig. 2), on the steep walls of the

162 Montségur edifice or in cracks at its base (Fig. 1C), to account for spatial variability of vent

163 assemblages. Eight of them, named "experimental quadrats", were devoted to the study of

164 recolonisation processes following faunal clearance after 1 (C1) and 2 (C2) years (August 2018

165 and June 2019 respectively). Replicate samples for each year were denoted as "a" or "b" (Fig.

166 1C). In addition to the experimental quadrats, five "reference" quadrats (R) were deployed

167 and sampled in 2017 (R0a, R0b), 2018 (R1) and 2019 (R2, R2cg) to characterise the natural

168 dynamics of faunal communities on Montségur throughout the experiment. The role of large

169 mobile predators (crabs, shrimp or fish) on local recolonisation was examined by covering

170   some of the pyramidal structures with a 1 cm plastic mesh. These specific quadrats were

171   denoted as "cg'' for caged (Fig. 2C). This experimental design is summarised in Figure 3.

172

2.3. Environmental characterisation

174   Temperature and key chemical parameters were assessed from *in situ* measurements on all

175   quadrats before and after faunal sampling and this, for each year of the study (2017 to 2019).

176   Our objectives were to identify the spatial and temporal variability of these factors and

177   evaluate their role in the recolonisation processes. The *in situ* chemical analysers CHEMINI

178   (Vuillemin et al., 2009) were used on three replicate points in each quadrat to measure

179   dissolved concentration of total sulphides [TdS : $H_2S+HS^-+S_2$] and total dissolved iron [TdFe :

180   Fe (II)]. To complete the chemical characterisation, water samples were collected with the

181   PEPITO water sampler at each quadrat prior to faunal sampling (Sarradin et al., 2009). Oxygen

182   concentrations were measured using an Aanderaa optode probe (Tengberg et al. 2006)

183   connected to the outlet of the PEPITO sampler. Methane [CH_4], was analysed back in the

184   laboratory by GC-FID and HID (Donval et al. 2008). In addition to this one-time yearly

185   characterisation, temperature was monitored every 2 hours over the deployment period using

186   two iButtons^{TM} probes attached to each quadrat and deployed directly on the mussel

187   assemblages with a measurement resolution of 0.5 °C.

188

2.4. Faunal sampling and identification

190   During the Momarsat 2017 cruise, eight experimental quadrats -noted "C"- were cleared of

191   their fauna using both the suction sampler and the claw of the ROV *Victor6000* mechanical

192   arm (Fig. 2A, 2B). The same year, R0a and R0b reference quadrats were also sampled, leading

193   to a total of 10 quadrats used to describe the pre-disturbed vent community of Montségur

194   (Fig. 3). During Momarsat 2018, the four experimental quadrats dedicated to the "one-year

195   after disturbance recolonisation study" -noted "C1"- and reference quadrat R1 were sampled

196   (5 quadrats in total; Fig. 3). During the Momarsat 2019 cruise, the four experimental quadrats

197   dedicated to the "two-year after disturbance recolonisation study" noted "C2"-and reference

198   quadrats R2 and R2-cg were sampled (6 quadrats, Fig. 3). The surface area of each quadrat

199   was filmed before and after faunal sampling with the ROV high definition cameras to estimate

200   the sampled surfaces using imagery analysis (Fig. 2A, 2B). A target with 7 mm checkerboard

201   squares was fixed on each quadrat, providing scaling in the field of view (Fig. 2B).

202   In this study, fauna will include macrofauna and any meiofauna taxa larger than 250 μm

203   (nematodes, copepods and ostracods). We also include species often considered as

204   megafauna (shrimp, mussels) recovered within the quadrats. The faunal samples were

205   preserved in 96% ethanol. All individuals collected were identified to the lowest possible

206   taxonomic level under a stereomicroscope and counted.

207   2.5. Population size structure

208   Size-frequency distributions of the six most dominant species were analysed for each sample

209   of the Montségur edifice. Each individual was measured, using different measurements

210   depending on the species (see details in Table S1). The biggest individuals were measured

211   using a caliper while small individuals were measured on screen to the nearest 0.001 mm,

212   using the Leica Application Suite software. Measurement error was calculated as the

213   maximum difference among 10 measurements of the same individual on 10 specimens

214   comprising a range of all sizes for each species (Table S1). For each assemblage sampled,

215   length-frequency distribution was plotted for the six species. Size class intervals were chosen

216   according to three criteria: i) most size-classes must have at least five individuals; ii) the

217   number of adjacent empty classes must be minimised; and iii) the interval has to be greater

218   than the measurement error (see Jollivet et al. 2000). Size-frequency distributions were

219   compared to a normal distribution using a one-sample Kolmogorov-Smirnov test and

220   differences between the pre-disturbed and post-disturbance communities were identified

221   using a pairwise Kolmogorov-Smirnov test. Non-parametric Wilcoxon-Mann-Whitney tests

222   were performed to identify differences in mean individual size between the pre-disturbed

223   community and the novel one, after the recolonisation processes in each location.

224   2.6. Data analyses

225   All analyses were computed in R environment (R Core Team, 2018). Species rarefaction curves

226   were computed for each sample, habitat and year to verify the robustness of the sampling

227   effort and characterise the overall diversity. Local diversity was estimated for each assemblage

228   by computing α-diversity indices such as species richness (S), Shannon entropy (H) and the

229   Pielou's evenness index (J') using the vegan package in R (Oksanen et al., 2019). Contingency

230 tables were weighted by the sampling surface for each quadrat for comparison purposes. The
231 resulting density data were used for all subsequent analyses.

232 **Environmental conditions** – The temperatures measured by the iButtons^{TM} probes were used
233 to characterise each assemblage/quadrat. Four temperature parameters were compiled,
234 including the average (T.avg), minimum (T.min), maximum (T.max) and standard deviation
235 (T.sd). In addition, average concentrations of oxygen (O_2), methane (CH_4), total dissolved iron
236 (TdFe) and sulphides (TdS) as well as standard deviations of TdFe and TdS were used to
237 characterise the spatial variability of abiotic factors among the different Montségur quadrats.
238 A principal component analysis (PCA) was built with all environmental variables (packages
239 FactoMineR and factoextra - Kassambara and Mundt 2019) to identify patterns in
240 environmental conditions among quadrats and determine which variables accounted for most
241 of the observed variance. Finally, Whittaker-Robinson periodograms, programmed in the R
242 package adespatial (Dray et al., 2020) were used to screen for significant periodicities in
243 temperature time series.

244 **Community structure** – A canonical redundancy analysis (RDA) was performed on Hellinger-
245 transformed densities and environmental variables retained by a forward selection (vegan
246 package - Oksanen et al. 2019) to evaluate the spatial variability of community composition in
247 relation to abiotic factors in the baseline communities on the Montségur edifice. This allows
248 us to evaluate the representativeness of baseline communities in Montségur in comparison
249 with faunal assemblages already described on other active edifices of the Lucky Strike vent
250 field.

251 **Recovery patterns** – Faunal recovery patterns were assessed from experimental quadrats.
252 Differences in faunal composition among quadrats along the recolonisation processes were
253 tested using a non-parametric analysis of similarity (ANOSIM; Anderson 2001). The ANOSIM R
254 value is based on differences in average ranking of dissimilarity indices (i.e. Bray-Curtis
255 dissimilarity matrix) between and within the different predefined groups (here each recovery
256 stage, i.e.: pre-disturbed state, one year and two years after disturbance). A RDA on Hellinger-
257 transformed densities data was also used to identify the role of environmental conditions and
258 biotic interactions (i.e. by testing the cage effect) on the structure of macrofaunal assemblages
259 during the recolonisation processes. A variable named "quadrat" was used to evaluate the
260 independence of the samples from the same quadrat over the years in the explanatory

261   environmental matrix. Moreover, to test for the effect of time after disturbance, we coded a

262   quantitative variable named "Yr-aft-dist" (i.e. year after disturbance). In this framework, pre-

263   disturbed reference samples were considered as baseline communities at an equilibrium state

264   and thus were coded with a value greater than 2 years. As the age of the natural community

265   is unknown, analyses were run with different values [3 years, 10 years and 100 years] but they

266   all yielded to similar results. Based on previous studies about the temporal stability of these

267   communities (more than 14 years on Eiffel Tower, Cuvelier et al. 2011b) and data about

268   recovery time in other vent system after a major disturbance (4-5 years, Gollner et al. 2017),

269   we considered 10 years as a good compromise to be used for the analysis.

270

3. Results

3.1.   Environmental conditions

273   Mean temperature among the different quadrats of Montségur varied between 5.2 °C and 9.5

274   °C (Table 1). R1 and C2a exhibited the highest maximum temperatures (with maximum of 16.1

275   °C and 22.1 °C respectively), but also higher concentrations in TdFe and CH_4 associated with a

276   more acidic pH (Table 1, Fig. S1).

277   The two temperature probes separated by ~ 10 cm deployed on each quadrat were used to

278   characterise the spatial variability of abiotic conditions at fine scales. While homogeneous

279   temperatures are observed within some quadrats (e.g. C1a, C1bcg, C2b, C2bcg), others

280   showed a high variability of temperatures in the narrow spatial gradient (few centimetres, e.g.

281   C1b, C2acg); (Fig. S2).

282   Notable differences in temperature on single quadrats between the two years were observed.

283   C1b, C1acg and C2a quadrats showed a sharp decrease in mean and variability of

284   temperatures at different times during the first year of deployment (Fig. S2). Periodogram

285   analyses carried out on temperature time series revealed significant periods of 12 h for most

286   quadrats. In addition, significant periods of 24 h were also identified on all quadrats except

287   C1acg. Additional periodic signals, possibly harmonics related to the tidal signal, with periods

288   of 36 h and 48 h, were also revealed for C1a, C1acg and C1bcg.

3.2. Pre-disturbed communities

The rarefaction curves built for each pre-disturbed sample of Montségur (Fig. S3) nearly reached an asymptote showing that the sampling effort was sufficient to capture the overall taxonomic diversity of macrofaunal benthic communities of active vent habitats. In total, 43 taxa were identified among a total of 34 158 individuals in the different samples. Most assemblages were characterised by a taxonomic richness varying between 19 and 28 (Table S2). The C1a sample, which is the only quadrat located on the west side of the edifice, displayed the highest taxonomic richness with the occurrence of 32 taxa, while R2 showed only 12 taxa among 133 identified specimens (Fig. 4; Table S2). Macrofaunal communities were dominated by six taxa: the engineer species *Bathymodiolus azoricus* and its commensal worm *Branchipolynoe seepensis*, the polychaete *Amphisamytha lutzi* and three species of gastropods *Lepetodrilus atlanticus*, *Protolira valvatoides* and *Pseudorimula midatlantica*. Together, they accounted for 68.3 ± 15.7% of the total abundance. The nematode *Oncholaimus dyvae* and copepod *Aphotopontius sp.*, which are typical meiofaunal species, were also abundant in the > 250 μm fraction of most samples. In the pre-disturbed community, ~74% of taxa (e.g. 29 taxa over 43) showed low occurrence and abundance (i.e. below 1% frequency) in the different samples (Table S3).

A RDA has been performed to identify the role of environmental conditions on faunal distribution and verify the temporal stability of baseline communities. The RDA model performed on Hellinger-transformed species densities accounted for 49.6% (adjusted R^2: 25.1%, p = 0.008) of the total inertia in macrofaunal species assemblage structure (Fig. 5). The overall RDA model was significant (*p-value* = 0.004) and only the first axis was significant (p = 0.05), accounting for 20% of the variation in community structure. Maximum temperature (T.max) and total dissolved sulphide concentrations (TdS) were the significant environmental factors influencing macrofaunal composition (p = 0.009 and 0.021, respectively). The years at which the samples were collected did not explain the differences between quadrats. R2cg sample stood out from the other sampling locations and was characterised by a high relative density of the gastropod *Lurifax vitreus*, contrasting with a low density of *B. azoricus* (Fig. 5). Moreover, the C2acg and R0b samples, characterised by a high density of amphipods (*Luckia striki*), formed a distinct group (Fig. 5). All other samples showed a quite homogeneous faunal composition.

3.3.   Recovery patterns of benthic communities

Recolonisation dynamics of the foundation species – The recovery rate of *Bathymodiolus azoricus*, in terms of density, varied between 9.7% and 37.6% on the different quadrats one year after disturbance, and from 1.9% to 33% two years after disturbance (Fig. 6). No significant difference can be noticed between the mean recovery rate after 1 year (19.8 ± 13%) and 2 years of recolonisation (14.4 ± 13.5%) (Student test: t = 0.59, *p-value* = 0.58). However, with the exception of the C2bcg quadrat, the percentage of recovery was slightly higher in the quadrats that were caged during the recolonisation process (>20%) compared to the uncaged quadrats (<15%) (Fig. 6). The size population structure analyses of *B. azoricus* showed individuals ranging from 251 µm to 8.5 cm length within the different assemblages (Fig. 6). The pre-disturbed structure of the population on Montségur showed a polymodal size distribution dominated by a large proportion (i.e. 52% of the overall population) of small individuals below 5 mm in shell-length and a tail of distribution in larger sizes containing several cohorts (Fig. 6). Pairwise Kolmogorov-Smirnov distribution tests showed significant differences in population size structure between the pre-disturbed and post-disturbance communities in all samples (*p-value* < 0.001), except C2b (D = 0.10, *p-value* = 0.13) (Fig. 6). Furthermore, Wilcoxon-Mann-Whitney tests highlighted that the mean shell length of *B. azoricus* was smaller 1 and 2 years after the disturbance compared to that of the pre-disturbed community for all samples except C1a and C2b (Fig. 6). Furthermore, the proportion of juveniles of *B. azoricus* (< 5 mm) in the overall population was higher in assemblages sampled 1 year (67%) and two years (70%) after the disturbance in comparison to pre-disturbed populations (52%) (Table S3).

Recolonisation dynamics of active vent communities – The rarefaction curves did not level off for most of the post-disturbance samples on Montségur, but they show similar trends than that of pre-disturbed communities (Fig. S3). The shape of the curves indicate that they should reach a plateau earlier, highlighting a higher evenness in the recovering communities. Species richness (S) is lower (from 1 to 6 less species) in the post-disturbance assemblages compared to the pre-disturbed communities 1 year after the induced disturbance (Fig. 4A, Table S2). On the other hand, two years after, the C2a and C2acg quadrats showed a higher species richness than pre-disturbed quadrats, while C2b and C2bcg exhibited lower values after the disturbance (Fig. 4A, Table S2). Overall, species richness was homogeneous between all samples and was not significantly different along the recolonisation process (Kruskal-Wallis

352   test: P= 1.17, *p-value* = 0.56, Fig. 4A). However, macrofaunal densities were significantly lower

353   after 1 year (15 768 ± 12 487 ind.m^{-2}) and 2 years (11 190 ± 8 270 ind.m^{-2}) after the

354   disturbance, in comparison to the pre-disturbed community (34 402 ± 7 590 ind.m^{-2}) (Kruskal-

355   Wallis test: P= 7.65, *p-value* = 0.021 and Post hoc Dunn test: *p-value* < 0.05, Fig. 4A) with a

356   density recovery rate ranging from 15.7% on C1b after 1 year to 79.6% on C2acg 2 years after

357   the disturbance (Fig. 6, Table S2). The Shannon index and Pielou's evenness were highly

358   variable across samples in the pre-disturbed communities, but higher 1 year and 2 years after

359   the disturbance (Fig. 4C and 4D, Table S2). Overall Pielou's evenness index is significantly

360   higher in post-disturbance communities compared to pre-disturbed communities (Kruskal-

361   Wallis test: P= 7.34, *p-value* = 0.026 and Post hoc Dunn test: *p-value* < 0.05, Fig. 4D). In the

362   same way, the proportion of low occurrence species is lower in post-disturbance communities

363   (60% after 1 year and 58% after 2 years) than prior to the induced disturbance (74%) (Table

364   S2).

365   The output of the RDA computed on Hellinger-transformed densities of the different species

366   along the recolonisation process showed a significant difference in faunal composition

367   between the pre-disturbed communities and post-disturbance communities at Montségur

368   (Fig. 7). The RDA model explained 42% (Adjusted R^2 = 20.5%) of the total inertia in species

369   assemblage structure (*p-value* = 0.006). The main driver of this observed difference is time

370   after the induced disturbance (*p-value* = 0.001), whereas no significant cage effect or

371   dependence between sites were observed (p-values = 0.300 and 0.262, respectively). The

372   analysis of similarity (ANOSIM) on Bray-Curtis dissimilarity matrix suggests a major change in

373   macrofaunal composition between pre-disturbed communities and those after 1 and 2 years

374   of recolonisation (R = 0.712, *p-value* = 0.001). However, no significant difference in faunal

375   composition was identified between the assemblages collected 1 year and those collected 2

376   years after the disturbance.

377   Some species appeared to play a major role in the observed differences along the

378   recolonisation process (Fig. 8). Indeed, a decrease in the abundance of the typical vent species

379   (*Bathymodiolus azoricus*, *Branchipolynoe seepensis*, *Amphisamytha lutzi* and *Lepetodrilus*

380   *atlanticus)* was observed in the post-disturbance communities, while small gastropod species

381   (i.e. *Lurifax vitreus*, *Protolira valvatoides*, *Laeviphitus desbruyeresi*, *Xylodiscula analoga*) and

382   nematodes (*Oncholaimus dyvae*) showed a significant increase in the post-disturbance

communities (Fig. 8, Fig. S4). *Pseudorimula midatlantica* and the copepod *Aphotopontius sp.* displayed higher relative abundances in the first year after the disturbance in comparison to the pre-disturbed community and returned to lower values 2 years after the disturbance. As observed for *B. azoricus,* the other dominant species displayed a polymodal structure of size distribution and differences have been identified between the pre-disturbed community and post disturbance state (pairwise Kolmogorov-Smirnov test) (Fig. S4). Furthermore, individuals of *A. lutzi*, *B. seepensis*, *L. lepetodrilus* and *P. valvatoides* were overall smaller within the communities after disturbance in comparison to those of the pre-disturbed community in most quadrats (Fig. S4). For *P. midatlantica*, only 1 quadrat showed significant differences in population size structure (Fig. S4).

4. Discussion

In this study, we provide an early evaluation of the recovery of deep-sea benthic communities to a small-scale (<1 m²) disturbance experiment at an active hydrothermal edifice located on the Lucky Strike vent field. The structure of pre-disturbed communities and their recovery patterns were characterised through the analysis of faunal composition, diversity, population size structure in relation to biotic and abiotic factors at the Montségur edifice. This experimental design represents an innovative approach to assess the recovery of vent communities in areas where opportunities to observe natural disturbances are rare. It provides useful insights about local recolonisation drivers at hydrothermal vents, data that can contribute to the elaboration of conservation strategies in the context of potential deep-sea mining activities on seafloor massive sulphides.

4.1. Habitat characterisation

In active vent ecosystems, environmental factors are strongly linked to the output flux and chemistry of hydrothermal fluids and the resulting physico-chemical conditions along the mixing gradient between vent fluids and surrounding sea water. Within the active habitats sampled in this study, mean temperature among *Bathymodiolus azoricus* faunal assemblages varied from 5.2 to 9.5 °C with a maximum of 22.1 °C, which corresponds to the temperature ranges of Eiffel Tower habitats (Husson et al. 2017, Sarrazin et al. 2020). We identified two microhabitats hosting *B. azoricus* assemblages, which have previously been described as cold and warm habitats in Sarrazin et al. (2015). However, while in our study these habitats are

colonised by mussels, in the previous study warm habitats were rather reported to be associated with shrimp assemblages. This discrepancy could be related to temperature measurements: in the present study, temperature was measured using iButtons[TM] deployed on or within the mussels while most measurements reported previously were conducted using the ROV probe placed a few millimeters above the faunal assemblages (Cuvelier et al. 2014a, Husson et al. 2017, Sarrazin et al. 2015, 2020). The rapid mixing of the warm fluids with the above cold seawater can account for these differences. Similar to previous studies, most samples belonging to the cold habitat showed small variability in environmental conditions and were associated with low temperature, low concentrations of iron and sulphides, high pH and high concentrations of dissolved oxygen (Cuvelier et al. 2011a; Sarrazin et al. 2015). However, a few quadrats (R1, C2a and R0b) were characterised by higher temperatures, total dissolved sulphide and iron concentrations as well as lower dissolved oxygen concentrations with acidic pH, which are more representative of warm habitats.

The continuous bi-hourly monitoring of temperature revealed a high spatial variability in temperature regime (up to 3°C across 10 cm), suggesting the occurrence of multiple microhabitats within a single quadrat. This was supported by high standard deviation values of replicate measurements for sulphides and iron concentrations performed every year. This small-scale temporal variability of temperature can be a result of several processes, including the interplay between sulphide and oxygen biological uptake (Johnson et al., 1988), the formation of diffuse fluids in the subsurface, the chemical reactivity of the mixing zone, the porosity of the substratum in active habitats on the East Pacific Rise (Butterfield et al. 1990; Sarrazin et al. 2002, Le Bris et al. 2006) or tidal oscillations (Barreyre et al. 2014). Our results show significant semi-diurnal and diurnal periods and harmonics, supporting the presence of periodic oscillations related to tidal processes. Tidal modulation of diffused-flow has been reported in many vent systems (Cuvelier et al., 2014b; Sarrazin et al., 2014; Scheirer et al., 2006). These variations are mainly caused by tidally induced currents (Barreyre et al., 2014; Khripounoff et al., 2008) and changes in hydrostatic pressure on the seafloor (Davis and Becker, 1999). This periodicity could be beneficial for symbiotic sessile species that need alternative inputs of reduced compounds and oxygen to ensure chemosynthesis (Scheirer et al. 2006, Mat et al. 2020) but can also influence the behaviour of mobile species (Lelièvre et al., 2017).

446

4.2. Pre-disturbed communities and natural variability

448

On the active Montségur edifice, all experimental quadrats were visually dominated by medium-sized *B. azoricus* mussels from 5.2 ± 8.8 mm to 24.4 ± 14.3 mm. These sizes are consistent with the mean lengths reported by Comtet and Desbruyères (1998) on different edifices of Lucky Strike (between 5.63 ± 5.67 mm and 49.63 ± 31.41 mm), but smaller than those measured by Sarrazin et al. (2015) on the nearby Eiffel Tower edifice (between 22.7 ± 18.07 and 74.7 ± 2.57 mm). Indeed, we observed a high proportion (between 52 and 96%) of very small individuals -below 3 mm- in each sample, sizes that correspond to post larval and juvenile stages. The presence of several successive cohorts suggests the occurrence of a massive recruitment event around June, just before sampling. These results are consistent with the lifecycle of *B. azoricus*, with an annual spawning event in January followed by a planktotrophic larval development and the settlement of post-larvae in May-June (Colaço et al., 2006; Comtet and Desbruyères, 1998; Dixon et al., 2006). Furthermore, differences in mean shell length of *B. azoricus* observed among samples on pre-disturbed communities may be due to spatial segregation of sizes related to environmental factors (Sarrazin et al., 2015; Husson et al., 2017) or to biotic interactions (e.g. competition, predation) that may play an important role in recruitment success and survival of post-larvae (Lenihan et al., 2008; Sancho et al., 2005).

466

All samples collected at the active Montségur edifice were dominated by the same macrofaunal species (e.g. *B. azoricus*, *B. seepensis*, *A. lutzi*, *P. valvatoides* and *L. atlanticus*), which have been previously described as indicator species of cold microhabitats on the Eiffel Tower edifice situated ~ 50 m from Montségur (Sarrazin et al., 2015b). The high similarity between the fauna from the two edifices may be related to their belonging to the same chemistry domain (Chavagnac et al. 2018, Sarrazin et al. 2020). Among the 43 macrofaunal species identified on Montségur, approximately 74% exhibit a low frequency of abundance (<1%). Total densities of organisms in the pre-disturbed communities ranged from 3 330 to 68 960 ind.m^{-2} across the different samples, and is much lower than the values reported by Sarrazin et al. (2020) on the same edifice (between 62 253 and 126 437 ind.m-2). In several studies, small mussel assemblages, inhabiting cold microhabitats, harbour higher density and

478 diversity of associated species than large mussel assemblages, found in warmer microhabitats

479 (Cuvelier et al., 2009; Dreyer et al., 2005; Sarrazin et al., 2015). Surprisingly, in this study the

480 highest densities of organisms have been observed in the warmest and more variable habitats.

481 This result may be linked to the differences in the method for assessing temperature as

482 mentioned above. Indeed, temperature values obtained by probes deployed directly on the

483 substratum are expected to be higher than the ones obtained with the ROV probe a few

484 millimeters above faunal assemblages.

485

486 As expected, macrofaunal distribution was significantly influenced by environmental

487 conditions, especially by mean temperature and mean concentrations in total sulphides and

488 methane, in addition to slightly acidic conditions (pH <7.3). However, biotic factors such as

489 competition for space and food resource, but also predation or facilitation, may also play an

490 important role in faunal distribution in diffuse flow habitats (Sarrazin et al. 1997, Sen et al.

491 2013; Gollner et al. 2015b; Husson et al. 2017). On the other hand, faunal composition within

492 reference quadrats did not differ over the three years of the experiment, suggesting a relative

493 stability of the community over time. This supports the observed high stability of mussel

494 communities on the nearby Eiffel Tower edifice, which led to the assumption that *B. azoricus*

495 assemblages at Lucky Strike can be considered as a "climax" community (Cuvelier et al.,

496 2011b). The absence of natural changes in faunal assemblages, at the edifice scale, during the

497 experiment allows us to use them as a baseline to test the effect of the induced disturbance

498 on benthic communities.

499

500   4.3. Recolonisation processes and recovery

501

502 In Figure 9, we propose a succession model of nMAR vent communities based on the present

503 experiment at the Lucky Strike vent field and from previous studies conducted after natural

504 disturbances at vents. The first step after the disturbance relies on the release of an ecological

505 niche induced by the removing of faunal assemblages. Then, the stabilisation of

506 environmental conditions, especially of temperature and reduced compounds, would allow

507 chemoautotrophic primary production and proliferation of microbial mats, as observed in

508 studies from vents in the Pacific Ocean (Marcus et al., 2009; Shank et al., 1998; Tunnicliffe et

509 al., 1997). This is followed, within one year, by the arrival of mobile opportunistic species,

510   including shrimps and copepod species. Although not significant, our results suggest that

511   these predator species may slow down the settlement of associated species, resulting in a

512   poor recovery of faunal densities despite a good species richness recovery. Two years after

513   the disturbance, the settlement of several gastropod species grazing on free-living microbial

514   mats have been observed. At this stage, the higher Pielou's evenness compared to baseline

515   communities suggests that biotic interactions are not yet fully effective within assemblages.

516   Gastropods have already been described as main pioneer colonists at 9°N EPR after the 2006

517   volcanic eruption (Mullineaux et al., 2012, 2010). Indeed, despite contrasting reproductive

518   characteristics, some of them are able to maintain an important effective population size and

519   support high abundances, especially through an early maturity and continuous gametogenesis

520   (Marticorena et al., 2020). Thereafter, we hypothesise a later settlement of the foundation

521   species *B. azoricus* due to its seasonal reproduction, which leads to a single recruitment event

522   in June (Colaço et al., 2006; Dixon et al., 2006). The recolonisation of *B. azoricus* can occur

523   through recruitment events and settlement of post-larvae and juveniles or by immigration of

524   mobile adults from nearby assemblages (Comtet and Desbruyères, 1998). Indeed,

525   observations made on imagery on the Eiffel Tower edifice showed that *B. azoricus* is able to

526   move several centimetres a day (Matabos, Sarrazin, unpublished data). Since the growth rate

527   of B. azoricus juveniles has been estimated to reach ~ 2 mm per year on the Eiffel Tower edifice

528   (from imagery analysis, Sarrazin and Matabos unpublished data), we can assume that the

529   presence of mussels larger than 1 cm after 1 and 2 years of recolonisation is most probably a

530   result of adult migration. On the other hand, the mean shell length of *B. azoricus* was

531   significantly lower and a higher proportion of juveniles were observed on post-disturbance

532   assemblages compared to pre-disturbed communities. This suggests that within our study, the

533   recruitment and settlement of young mussels were the main drivers of recolonisation after

534   the disturbance, rather than migration. Moreover, the results of the predator exclusion

535   experiment suggest that the recruitment success of *B. azoricus* might depend on predation

536   pressure on post-larval individuals by large mobile predators (e.g. shrimp, crabs, fishes). The

537   impact of predation on the entire benthic community could be even more significant when

538   predators specifically feed on taxa that play a key role in the community and interact widely

539   with other species (Paine, 1966). We also observed that the cages led to the formation of thick

540   microbial mats on their surfaces, implying that the presence of the plastic mesh and its size

541   may have modified the input of hydrothermal fluids. The deployment of additional "true" cage

control quadrats would be necessary to dissociate the role of predator exclusion and potentially other effects of the mesh such as hydrodynamic modifications. The establishment and growth of *B. azoricus* may then promote the settlement of low occurrence species and a rapid recovery of faunal densities through the creation of a three dimensional habitat that contributes to reduce fluid flux, making the habitat more suitable for other species (Johnson et al. 1988; Sarrazin et al. 1997, Shank et al. 1998). Finally, biotic interactions including predation, competition for space and nutritional resources and facilitation may lead to changes in faunal relative abundance and dominance before reaching an equilibrium. All these mechanisms contribute to reducing the evenness among assemblages and enhance the dominance of a few taxa (Fig. 9). Once this equilibrium is achieved, we can consider that these assemblages reach their climax. The climax community of Montségur appears to be similar to that of the neighbouring Eiffel Tower edifice (Cuvelier et al., 2011a) and some other active edifices of the Lucky Strike vent field (Sarrazin et al. 2020). These communities are characterised by the dominance of a few vent taxa and a high proportion of low occurrence species. Natural or anthropogenic disturbance events, which can occur at each step of this successional model, may lead to significant changes in faunal assemblages and even provoke community collapse, depending on their spatial breadth as proposed in different vent successional models (Sarrazin et al. 1997, Shank et al. 1998).

Several factors can come into play in recolonisation and ecological succession following a disturbance, and their relative importance changes according to the scale of disturbance (Zajac et al. 1998, Benedetti 2000). After a small-scale disturbance, recovery of vent assemblages are strongly affected by the spatio-temporal variability of environmental conditions, which may lead to local extinction or creation of new suitable habitats (Sarrazin et al. 1997; Shank et al. 1998, Marcus et al. 2009; Sen et al. 2014). Feeding strategies (Lelièvre et al. 2018; Van Audenhaege et al., 2019) and biotic interactions (i.e. competition for space, facilitation or predation) have also been identified as important drivers of faunal succession at the edifice scale (Sarrazin et al. 1997, Micheli et al. 2002; Hunt et al. 2004; Govenar and Fisher 2007; Cuvelier et al. 2014a). In this study, we showed that, at this small-scale, biological interactions are more likely to play a predominant role in faunal succession rather than environmental conditions. The same observations have been noticed on vents at back-arc basins and may be due to the high stability of environmental conditions, typical of slow-spreading centers (Sen et al., 2014). Furthermore, in mosaic habitats, the diversity and species

composition at the boundary of disturbed patches might modulate biotic interactions and migrations of individuals, influencing early stages of recovery (Bulleri et al. 2006). However, diversity descriptors and faunal composition were relatively homogeneous between the different quadrats at each step of the recolonisation process, suggesting that succession after small-scale disturbance at Lucky Strike can be described as a deterministic sequence of species replacement. As observed on rocky-shore habitats, the timing of disturbance might also affect recolonisation patterns (Sousa 1985, Benedetti and Cinelli 1996). For example, *B. azoricus* have been described to recruit seasonally around the month of June (Dixon et al. 2006; Colaço et al. 2006) and the occurrence of disturbance in spring might result in a faster recovery of assemblages and less importance of gastropods in the first stage of recolonisation.

5. Conclusion

We designed a novel *in situ* experimental approach to identify biotic and abiotic factors driving the recolonisation and succession of vent communities after a small-scale disturbance. Recolonisation dynamics was strongly affected by species composition of the neighbouring faunal assemblages. Biotic interactions were predominant and highly influenced the slow recovery of vent assemblages, while environmental factors remained stable. Our results, coupled with observations from literature data, lead to a first conceptual model of colonisation and ecological succession for northern Mid-Atlantic communities.

At regional scales (i.e. vent field), life-history traits including reproduction (Kelly and Metaxas, 2007), larval dispersal modes and recruitment abilities (Levin et al., 1996; Levin, 2006; Mullineaux et al., 2003, 2012) constitute additional key factors that influence faunal colonisation processes and subsequent successional patterns (Zajac et al., 1998; Adams et al., 2012; Nakamura et al., 2014). While the recolonisation of areas following large-scale disturbance relies on dispersal across vent fields, at local scale the successful settlement of post-larvae depends on habitat suitability, environmental conditions and biotic interactions. Understanding the processes acting at small scales are paramount in evaluating mechanisms controlling successional dynamics after recolonisation by species from afar. In addition, recent workshops and working groups, emerging from the development of mining regulations and the necessity to inform industries and policy makers, stressed the urgent need to address

knowledge gaps in vent species biology and ecology (Collins et al. 2013; Levin et al. 2016; Dunn et al. 2018, ISA REMPS, SEMPIA). This study is one of the first to assess natural recovery of communities on a slow-spreading ridge and provide data that are essential to elaborate and develop conservation strategies and mitigate long-term harmful effects of anthropogenic activities on hydrothermal vent ecosystems.

DOI of cruises involved

SARRADIN Pierre-Marie, CANNAT Mathilde (2017) MOMARSAT2017 cruise, RV Pourquoi pas ?, https://doi.org/10.17600/17000500

CANNAT Mathilde (2018) MOMARSAT2018 cruise, RV L'Atalante, https://doi.org/10.17600/18000514

SARRADIN Pierre-Marie, LEGRAND Julien (2019) MOMARSAT2019 cruise, RV Pourquoi pas ?, https://doi.org/10.17600/18001110

Acknowledgements

References

Adams, D.K., Arellano, S.M., Govenar, B., 2012. Larval dispersal : vent life in the water column. https://doi.org/10.5670/oceanog.2012.24

Anderson, M.J., 2001. A new method for non-parametric multivariate analysis of variance. Austral Ecol. 26, 32–46. https://doi.org/10.1111/j.1442-9993.2001.01070.pp.x

643 Baco, A.R., Etter, R.J., Ribeiro, P.A., Heyden, S. von der, Beerli, P., Kinlan, B.P., 2016. A synthesis of
644 genetic connectivity in deep-sea fauna and implications for marine reserve design. Mol. Ecol. 25, 3276–
645 3298. https://doi.org/10.1111/mec.13689

646 Barreyre, T., Escartín, J., Sohn, R.A., Cannat, M., Ballu, V., Crawford, W.C., 2014. Temporal variability
647 and tidal modulation of hydrothermal exit-fluid temperatures at the Lucky Strike deep-sea vent field,
648 Mid-Atlantic Ridge. J. Geophys. Res. Solid Earth 119, 2543–2566.
649 https://doi.org/10.1002/2013JB010478

650 Beaulieu, S.E., Baker, E.T., German, C.R., 2015. Where are the undiscovered hydrothermal vents on
651 oceanic spreading ridges? Deep Sea Res. Part II Top. Stud. Oceanogr., Exploring New Frontiers in Deep-
652 Sea Research: In Honor and Memory of Peter A. Rona 121, 202–212.
653 https://doi.org/10.1016/j.dsr2.2015.05.001

654 Benedetti-Cecchi, L., Cinelli, F., 1996. Patterns of disturbance and recovery in littoral rock pools:
655 nonhierarchical competition and spatial variability in secondary succession. Marine Ecology Progress
656 Series 135, 145–161. https://doi.org/10.3354/meps135145

657 Benedetti-Cecchi, L., 2000. Predicting Direct and Indirect Interactions During Succession in a Mid-
658 Littoral Rocky Shore Assemblage. Ecological Monographs 70, 45–72. https://doi.org/10.1890/0012-
659 9615(2000)070[0045:PDAIID]2.0.CO;2

660 Boschen, R.E., Rowden, A.A., Clark, M.R., Gardner, J.P.A., 2013. Mining of deep-sea seafloor massive
661 sulfides: A review of the deposits, their benthic communities, impacts from mining, regulatory
662 frameworks and management strategies. Ocean Coast. Manag. 84, 54–67.
663 https://doi.org/10.1016/j.ocecoaman.2013.07.005

664 Breusing, C., Biastoch, A., Drews, A., Metaxas, A., Jollivet, D., Vrijenhoek, R.C., Bayer, T., Melzner, F.,
665 Sayavedra, L., Petersen, J.M., Dubilier, N., Schilhabel, M.B., Rosenstiel, P., Reusch, T.B.H., 2016.
666 Biophysical and Population Genetic Models Predict the Presence of "Phantom" Stepping Stones
667 Connecting Mid-Atlantic Ridge Vent Ecosystems. Curr. Biol. CB 26, 2257–2267.
668 https://doi.org/10.1016/j.cub.2016.06.062

669 Bulleri, F., Benedetti-Cecchi, L., 2006. Mechanisms of recovery and resilience of different components
670 of mosaics of habitats on shallow rocky reefs. Oecologia 149. https://doi.org/10.1007/s00442-006-
671 0459-3

672 Butterfield, D.A., Jonasson, I.R., Massoth, G.J., Feely, R.A., Roe, K.K., Embley, R.E., Holden, J.F., McDuff,
673 R.E., Lilley, M.D., Delaney, J.R., 1997. Seafloor eruptions and evolution of hydrothermal fluid chemistry.
674 Philos. Trans. R. Soc. Lond. Ser. Math. Phys. Eng. Sci. 355, 369–386.
675 https://doi.org/10.1098/rsta.1997.0013

676 Butterfield, D.A., Massoth, G.J., McDuff, R.E., Lupton, J.E., Lilley, M.D., 1990. Geochemistry of
677 hydrothermal fluids from Axial Seamount hydrothermal emissions study vent field, Juan de Fuca Ridge:
678 Subseafloor boiling and subsequent fluid-rock interaction. J. Geophys. Res. Solid Earth 95, 12895–
679 12921. https://doi.org/10.1029/JB095iB08p12895

680 Chavagnac, V., Leleu, T., Fontaine, F., Cannat, M., Ceuleneer, G., Castillo, A., 2018. Spatial Variations in
681 Vent Chemistry at the Lucky Strike Hydrothermal Field, Mid-Atlantic Ridge (37°N): Updates for
682 Subseafloor Flow Geometry From the Newly Discovered Capelinhos Vent. Geochemistry, Geophysics,
683 Geosystems 19, 4444–4458. https://doi.org/10.1029/2018GC007765

684 Childress, J.J., Fisher, C.R., 1992. The biology of hydrothermal vent animals: physiology, biochemistry,
685 and autotrophic symbioses. Unkn. J. 337–441.

686 Colaço, A., Martins, I., Laranjo, M., Pires, L., Leal, C., Prieto, C., Costa, V., Lopes, H., Rosa, D., Dando,
687 P.R., Serrão-Santos, R., 2006. Annual spawning of the hydrothermal vent mussel, Bathymodiolus
688 azoricus, under controlled aquarium, conditions at atmospheric pressure. J. Exp. Mar. Biol. Ecol. 333,
689 166–171. https://doi.org/10.1016/j.jembe.2005.12.005

690 Collins, P.C., Kennedy, R., Van Dover, C.L., 2012. A biological survey method applied to seafloor massive
691 sulphides (sms) with contagiously distributed hydrothermal-vent fauna.
692 https://doi.org/10.3354/meps09646

693 Comtet, T., Desbruyères, D., 1998. Population structure and recruitment in mytilid bivalves from the
694 Lucky Strike and Menez Gwen hydrothermal vent fields (37°17\'N and 37°50\'N on the Mid-Atlantic
695 Ridge). Mar. Ecol. Prog. Ser. 163, 165–177. https://doi.org/10.3354/meps163165

696 Connell, J.H., Keough, M.J., 1985. Disturbance and patch dynamics of subtidal marine animals on hard
697 substrata.

698 Corliss, J.B., Dymond, J., Gordon, L.I., Edmond, J.M., Herzen, R.P. von, Ballard, R.D., Green, K., Williams,
699 D., Bainbridge, A., Crane, K., Andel, T.H. van, 1979. Submarine Thermal Springs on the Galápagos Rift.
700 Science 203, 1073–1083. https://doi.org/10.1126/science.203.4385.1073

701 Cuvelier, D., Beesau, J., Ivanenko, V.N., Zeppilli, D., Sarradin, P.-M., Sarrazin, J., 2014a. First insights
702 into macro- and meiofaunal colonisation patterns on paired wood/slate substrata at Atlantic deep-sea
703 hydrothermal vents. Deep Sea Res. Part Oceanogr. Res. Pap. 87, 70–81.
704 https://doi.org/10.1016/j.dsr.2014.02.008

705 Cuvelier, D., Gollner, S., Jones, D.O.B., Kaiser, S., Arbizu, P.M., Menzel, L., Mestre, N.C., Morato, T.,
706 Pham, C., Pradillon, F., Purser, A., Raschka, U., Sarrazin, J., Simon-Lledó, E., Stewart, I.M., Stuckas, H.,
707 Sweetman, A.K., Colaço, A., 2018. Potential Mitigation and Restoration Actions in Ecosystems Impacted
708 by Seabed Mining. Front. Mar. Sci. 5. https://doi.org/10.3389/fmars.2018.00467

709 Cuvelier, D., Legendre, P., Laes, A., Sarradin, P.-M., Sarrazin, J., 2014b. Rhythms and Community
710 Dynamics of a Hydrothermal Tubeworm Assemblage at Main Endeavour Field – A Multidisciplinary
711 Deep-Sea Observatory Approach. PLOS ONE 9, e96924.
712 https://doi.org/10.1371/journal.pone.0096924

713 Cuvelier, D., Sarradin, P.-M., Sarrazin, J., Colaço, A., Copley, J.T., Desbruyères, D., Glover, A.G., Santos,
714 R.S., Tyler, P.A., 2011a. Hydrothermal faunal assemblages and habitat characterisation at the Eiffel
715 Tower edifice (Lucky Strike, Mid-Atlantic Ridge). Mar. Ecol. 32, 243–255.
716 https://doi.org/10.1111/j.1439-0485.2010.00431.x

717 Cuvelier, D., Sarrazin, J., Colaço, A., Copley, J., Desbruyères, D., Glover, A.G., Tyler, P., Serrão Santos,
718 R., 2009. Distribution and spatial variation of hydrothermal faunal assemblages at Lucky Strike (Mid-
719 Atlantic Ridge) revealed by high-resolution video image analysis. Deep Sea Res. Part Oceanogr. Res.
720 Pap. 56, 2026–2040. https://doi.org/10.1016/j.dsr.2009.06.006

721 Cuvelier, D., Sarrazin, J., Colaço, A., Copley, J.T., Glover, A.G., Tyler, P.A., Santos, R.S., Desbruyères, D.,
722 2011b. Community dynamics over 14 years at the Eiffel Tower hydrothermal edifice on the Mid-
723 Atlantic Ridge. Limnol. Oceanogr. 56, 1624–1640. https://doi.org/10.4319/lo.2011.56.5.1624

724 Davis, E., Becker, K., 1999. Tidal pumping of fluids within and from the oceanic crust: New observations
725 and opportunities for sampling the crustal hydrosphere. Earth Planet. Sci. Lett. 172, 141–149.
726 https://doi.org/10.1016/S0012-821X(99)00197-1

727 Denny, M.W., 1987. Lift as a mechanism of patch initiation in mussel beds. Journal of Experimental
728 Marine Biology and Ecology 113, 231–245. https://doi.org/10.1016/0022-0981(87)90103-1

729 Dixon, D.R., Lowe, D.M., Miller, P.I., Villemin, G.R., Colaço, A., Serrão-Santos, R., Dixon, L.R.J., 2006.
730 Evidence of seasonal reproduction in the Atlantic vent mussel Bathymodiolus azoricus, and an
731 apparent link with the timing of photosynthetic primary production. J. Mar. Biol. Assoc. U. K. 86, 1363–
732 1371. https://doi.org/10.1017/S0025315406014391

733 Donval, J.-P., Charlou, J.-L., Lucas, L., 2008. Analysis of light hydrocarbons in marine sediments by
734 headspace technique: Optimization using design of experiments. Chemometrics and Intelligent
735 Laboratory Systems 94, 89–94. https://doi.org/10.1016/j.chemolab.2008.06.010

736 Dray, S., Bauman, D., Blanchet, G., Borcard, D., Clappe, S., Guenard, G., Jombart, T., Larocque, G.,
737 Legendre, P., Madi, N., Wagner, H.H., 2020. adespatial: Multivariate Multiscale Spatial Analysis.

738 Dreyer, J.C., Knick, K.E., Flickinger, W.B., Dover, C.L.V., 2005. Development of macrofaunal community
739 structure in mussel beds on the northern East Pacific Rise. Mar. Ecol. Prog. Ser. 302, 121–134.
740 https://doi.org/10.3354/meps302121

741 Dunn, D.C., Dover, C.L.V., Etter, R.J., Smith, C.R., Levin, L.A., Morato, T., Colaço, A., Dale, A.C., Gebruk,
742 A.V., Gjerde, K.M., Halpin, P.N., Howell, K.L., Johnson, D., Perez, J.A.A., Ribeiro, M.C., Stuckas, H.,
743 Weaver, P., Participants, S.W., 2018. A strategy for the conservation of biodiversity on mid-ocean
744 ridges from deep-sea mining. Science Advances 4, eaar4313. https://doi.org/10.1126/sciadv.aar4313

745 Kassambara and Mundt, 2009. Factoextra: Extract and Visualize the Results of Multivariate Data
746 Analyses, 2019. , R package.

747 Gollner, S., Govenar, B., Arbizu, P.M., Mills, S., Le Bris, N., Weinbauer, M., Shank, T.M., Bright, M.,
748 2015a. Differences in recovery between deep-sea hydrothermal vent and vent-proximate communities
749 after a volcanic eruption. Deep Sea Res. Part Oceanogr. Res. Pap. 106, 167–182.
750 https://doi.org/10.1016/j.dsr.2015.10.008

751 Gollner, S., Riemer, B., Arbizu, P.M., Bris, N.L., Bright, M., 2010. Diversity of Meiofauna from the 9°50'N
752 East Pacific Rise across a Gradient of Hydrothermal Fluid Emissions. PLOS ONE 5, e12321.
753 https://doi.org/10.1371/journal.pone.0012321

754 Gollner, S., Govenar, B., Fisher, C.R., Bright, M., 2015b. Size matters at deep-sea hydrothermal vents:
755 different diversity and habitat fidelity patterns of meio- and macrofauna. Mar. Ecol. Prog. Ser. 520, 57–
756 66. https://doi.org/10.3354/meps11078

757 Gollner, S., Kaiser, S., Menzel, L., Jones, D.O.B., Brown, A., Mestre, N.C., van Oevelen, D., Menot, L.,
758 Colaço, A., Canals, M., Cuvelier, D., Durden, J.M., Gebruk, A., Egho, G.A., Haeckel, M., Marcon, Y.,
759 Mevenkamp, L., Morato, T., Pham, C.K., Purser, A., Sanchez-Vidal, A., Vanreusel, A., Vink, A., Martinez
760 Arbizu, P., 2017. Resilience of benthic deep-sea fauna to mining activities. Mar. Environ. Res. 129, 76–
761 101. https://doi.org/10.1016/j.marenvres.2017.04.010

762 Gollner, S., Govenar, B., Martinez Arbizu, P., Mullineaux, L.S., Mills, S., Le Bris, N., Weinbauer, M.,
763 Shank, T.M., Bright, M., 2020. Animal Community Dynamics at Senescent and Active Vents at the 9°N

764   East   Pacific   Rise   After   a   Volcanic   Eruption.   Front.   Mar.   Sci.   6.
765   https://doi.org/10.3389/fmars.2019.00832

766   Govenar, B., Fisher, C.R., 2007. Experimental evidence of habitat provision by aggregations of Riftia
767   pachyptila at hydrothermal vents on the East Pacific Rise. Mar. Ecol. 28, 3–14.
768   https://doi.org/10.1111/j.1439-0485.2007.00148.x

769   Hunt, H.L., Metaxas, A., Jennings, R.M., Halanych, K.M., Mullineaux, L.S., 2004. Testing biological
770   control of colonization by vestimentiferan tubeworms at deep-sea hydrothermal vents (East Pacific
771   Rise, 9°50′N). Deep Sea Res. Part Oceanogr. Res. Pap. 51, 225–234.
772   https://doi.org/10.1016/j.dsr.2003.10.008

773   Husson, B., Sarradin, P.-M., Zeppilli, D., Sarrazin, J., 2017. Picturing thermal niches and biomass of
774   hydrothermal vent species. Deep Sea Res. Part II Top. Stud. Oceanogr., Advances in deep-sea biology:
775   biodiversity, ecosystem functioning and conservation 137, 6–25.
776   https://doi.org/10.1016/j.dsr2.2016.05.028

777   Johnson, K.S., Childress, J.J., Beehler, C.L., 1988. Short-term temperature variability in the Rose Garden
778   hydrothermal vent field: an unstable deep-sea environment. Deep Sea Res. Part Oceanogr. Res. Pap.
779   35, 1711–1721. https://doi.org/10.1016/0198-0149(88)90045-3

780   Jollivet, D., Empis, A., Baker, M.C., Hourdez, S., Comtet, T., Jouin-Toulmond, C., Desbruyères, D., Tyler,
781   P.A., 2000. Reproductive biology, sexual dimorphism, and population structure of the deep sea
782   hydrothermal vent scale-worm, Branchipolynoe seepensis (Polychaeta: Polynoidae). Journal of the
783   Marine   Biological   Association   of   the   United   Kingdom   80,   55–68.
784   https://doi.org/10.1017/S0025315499001563

785   Kelly, N.E., Metaxas, A., 2007. Influence of habitat on the reproductive biology of the deep-sea
786   hydrothermal vent limpet Lepetodrilus fucensis (Vetigastropoda: Mollusca) from the Northeast Pacific.
787   Mar. Biol. 151, 649–662. https://doi.org/10.1007/s00227-006-0505-z

788   Khripounoff, A., Vangriesheim, A., Crassous, P., Segonzac, M., Lafon, V., Warén, A., 2008. Temporal
789   variation of currents, particulate flux and organism supply at two deep-sea hydrothermal fields of the
790   Azores   Triple   Junction.   Deep   Sea   Res.   Part   Oceanogr.   Res.   Pap.   55,   532–551.
791   https://doi.org/10.1016/j.dsr.2008.01.001

792   Langmuir, C., Humphris, S., Fornari, D., Van Dover, C., Von Damm, K., Tivey, M.K., Colodner, D., Charlou,
793   J.-L., Desonie, D., Wilson, C., Fouquet, Y., Klinkhammer, G., Bougault, H., 1997. Hydrothermal vents
794   near a mantle hot spot: the Lucky Strike vent field at 37°N on the Mid-Atlantic Ridge. Earth Planet. Sci.
795   Lett. 148, 69–91. https://doi.org/10.1016/S0012-821X(97)00027-7

796   Le Bris, N., Govenar, B., Le Gall, C., Fisher, C.R., 2006. Variability of physico-chemical conditions in
797   9°50′N   EPR   diffuse   flow   vent   habitats.   Mar.   Chem.   98,   167–182.
798   https://doi.org/10.1016/j.marchem.2005.08.008

799   Leibold, M.A., Holyoak, M., Mouquet, N., Amarasekare, P., Chase, J.M., Hoopes, M.F., Holt, R.D., Shurin,
800   J.B., Law, R., Tilman, D., Loreau, M., Gonzalez, A., 2004. The metacommunity concept: a framework for
801   multi-scale community ecology. Ecology Letters 7, 601–613. https://doi.org/10.1111/j.1461-
802   0248.2004.00608.x

803   Lelièvre, Y., Legendre, P., Matabos, M., Mihály, S., Lee, R.W., Sarradin, P.-M., Arango, C.P., Sarrazin, J.,
804   2017. Astronomical and atmospheric impacts on deep-sea hydrothermal vent invertebrates. Proc. R.
805   Soc. B Biol. Sci. 284, 319–407. https://doi.org/10.1098/rspb.2016.2123

806   Lenihan, H.S., Mills, S.W., Mullineaux, L.S., Peterson, C.H., Fisher, C.R., Micheli, F., 2008. Biotic
807   interactions at hydrothermal vents: Recruitment inhibition by the mussel Bathymodiolus
808   thermophilus. Deep Sea Res. Part Oceanogr. Res. Pap. 55, 1707–1717.
809   https://doi.org/10.1016/j.dsr.2008.07.007

810   Levin, L.A., 2006. Recent progress in understanding larval dispersal: new directions and digressions.
811   Integr. Comp. Biol. 46, 282–297. https://doi.org/10.1093/icb/icj024

812   Levin, L.A., Baco, A.R., Bowden, D.A., Colaco, A., Cordes, E.E., Cunha, M.R., Demopoulos, A.W.J., Gobin,
813   J., Grupe, B.M., Le, J., Metaxas, A., Netburn, A.N., Rouse, G.W., Thurber, A.R., Tunnicliffe, V., Van Dover,
814   C.L., Vanreusel, A., Watling, L., 2016a. Hydrothermal Vents and Methane Seeps: Rethinking the Sphere
815   of Influence. Front. Mar. Sci. 3. https://doi.org/10.3389/fmars.2016.00072

816   Levin, L.A., D, T., G, T., 1996. Succession of macrobenthos in a created salt marsh. Mar. Ecol. Prog. Ser.
817   141, 67–82. https://doi.org/10.3354/meps141067

818   Levin, L.A., Mengerink, K., Gjerde, K.M., Rowden, A.A., Van Dover, C.L., Clark, M.R., Ramirez-Llodra, E.,
819   Currie, B., Smith, C.R., Sato, K.N., Gallo, N., Sweetman, A.K., Lily, H., Armstrong, C.W., Brider, J., 2016b.
820   Defining "serious harm" to the marine environment in the context of deep-seabed mining. Mar. Policy
821   74, 245–259. https://doi.org/10.1016/j.marpol.2016.09.032

822   Luther, G.W., Rozan, T.F., Taillefert, M., Nuzzio, D.B., Di Meo, C., Shank, T.M., Lutz, R.A., Cary, S.C.,
823   2001. Chemical speciation drives hydrothermal vent ecology. Nature 410, 813–816.
824   https://doi.org/10.1038/35071069

825   Marcus, J., Tunnicliffe, V., Butterfield, D.A., 2009. Post-eruption succession of macrofaunal
826   communities at diffuse flow hydrothermal vents on Axial Volcano, Juan de Fuca Ridge, Northeast
827   Pacific. Deep Sea Res. Part II Top. Stud. Oceanogr., Marine Benthic Ecology and Biodiversity: A
828   Compilation of Recent Advances in Honor of J. Frederick Grassle 56, 1586–1598.
829   https://doi.org/10.1016/j.dsr2.2009.05.004

830   Marsh, L., Copley, J.T., Huvenne, V.A.I., Linse, K., Reid, W.D.K., Rogers, A.D., Sweeting, C.J., Tyler, P.A.,
831   2012. Microdistribution of Faunal Assemblages at Deep-Sea Hydrothermal Vents in the Southern
832   Ocean. PLoS One 7. https://doi.org/10.1371/journal.pone.0048348

833   Marticorena, J., Matabos, M., Sarrazin, J., Ramirez-Llodra, E., 2020. Contrasting reproductive biology
834   of two hydrothermal gastropods from the Mid-Atlantic Ridge: implications for resilience of vent
835   communities. Mar. Biol. 167, 109. https://doi.org/10.1007/s00227-020-03721-x

836   Mat, A.M., Sarrazin, J., Markov, G.V., Apremont, V., Dubreuil, C., Eché, C., Fabioux, C., Klopp, C.,
837   Sarradin, P.-M., Tanguy, A., Huvet, A., Matabos, M., 2020. Biological rhythms in the deep-sea
838   hydrothermal mussel Bathymodiolus azoricus. Nature Communications 11, 3454.
839   https://doi.org/10.1038/s41467-020-17284-4

840   Micheli, F., Peterson, C.H., Mullineaux, L.S., Fisher, C.R., Mills, S.W., Sancho, G., Johnson, G.A., Lenihan,
841   H.S., 2002. Predation Structures Communities at Deep-Sea Hydrothermal Vents. Ecol. Monogr. 72,
842   365–382. https://doi.org/10.1890/0012-9615(2002)072[0365:PSCADS]2.0.CO;2

843   Mullineaux, L.S., Adams, D.K., Mills, S.W., Beaulieu, S.E., 2010. Larvae from afar colonize deep-sea
844   hydrothermal vents after a catastrophic eruption. Proc. Natl. Acad. Sci. 107, 7829–7834.
845   https://doi.org/10.1073/pnas.0913187107

846 Mullineaux, L.S., Metaxas, A., Beaulieu, S.E., Bright, M., Gollner, S., Grupe, B.M., Herrera, S., Kellner,
847 J.B., Levin, L.A., Mitarai, S., Neubert, M.G., Thurnherr, A.M., Tunnicliffe, V., Watanabe, H.K., Won, Y.-
848 J., 2018. Exploring the Ecology of Deep-Sea Hydrothermal Vents in a Metacommunity Framework.
849 Front. Mar. Sci. 5. https://doi.org/10.3389/fmars.2018.00049

850 Mullineaux, L.S., Bris, N.L., Mills, S.W., Henri, P., Bayer, S.R., Secrist, R.G., Siu, N., 2012. Detecting the
851 Influence of Initial Pioneers on Succession at Deep-Sea Vents. PLOS ONE 7, e50015.
852 https://doi.org/10.1371/journal.pone.0050015

853 Mullineaux, L.S., Peterson, C.H., Micheli, F., Mills, S.W., 2003. Successional Mechanism Varies Along a
854 Gradient in Hydrothermal Fluid Flux at Deep-Sea Vents. Ecol. Monogr. 73, 523–542.
855 https://doi.org/10.1890/02-0674

856 Nakamura, M., Watanabe, H., Sasaki, T., Ishibashi, J., Fujikura, K., Mitarai, S., 2014. Life history traits of
857 Lepetodrilus nux in the Okinawa Trough, based upon gametogenesis, shell size, and genetic variability.
858 Mar. Ecol. Prog. Ser. 505, 119–130. https://doi.org/10.3354/meps10779

859 Oksanen, J., Blanchet, F.G., Friendly, M., Kindt, R., Legendre, P., McGlinn, D., Minchin, P.R., O'Hara,
860 R.B., Simpson, G.L., Solymos, P., Stevens, M.H.H., Szoecs, E., Wagner, H., 2019. vegan: Community
861 Ecology Package.

862 Ondreas, H., Cannat, M., Fouquet, Y., Normand, A., Sarradin, P., Sarrazin, J., 2009. Recent volcanic
863 events and the distribution of hydrothermal venting at the Lucky Strike hydrothermal field, Mid-
864 Atlantic Ridge. Geochem. Geophys. Geosystems 10. https://doi.org/10.1029/2008gc002171

865 Orcutt, B.N., Bradley, J.A., Brazelton, W.J., Estes, E.R., Goordial, J.M., Huber, J.A., Jones, R.M.,
866 Mahmoudi, N., Marlow, J.J., Murdock, S., Pachiadaki, M., 2020. Impacts of deep-sea mining on
867 microbial ecosystem services. Limnol. Oceanogr. n/a. https://doi.org/10.1002/lno.11403

868 Paine, R.T., 1966. Food Web Complexity and Species Diversity. Am. Nat. 100, 65–75.

869 Sancho, G., Fisher, C.R., Mills, S., Micheli, F., Johnson, G.A., Lenihan, H.S., Peterson, C.H., Mullineaux,
870 L.S., 2005. Selective predation by the zoarcid fish Thermarces cerberus at hydrothermal vents. Deep
871 Sea Res. Part Oceanogr. Res. Pap. 52, 837–844. https://doi.org/10.1016/j.dsr.2004.12.002

872 Sarradin, P.-M., Waeles, M., Bernagout, S., Le Gall, C., Sarrazin, J., Riso, R., 2009. Speciation of dissolved
873 copper within an active hydrothermal edifice on the Lucky Strike vent field (MAR, 37°N). Sci. Total
874 Environ. 407, 869–878. https://doi.org/10.1016/j.scitotenv.2008.09.056

875 Sarrazin, J., Cuvelier, D., Peton, L., Legendre, P., Sarradin, P.M., 2014. High-resolution dynamics of a
876 deep-sea hydrothermal mussel assemblage monitored by the EMSO-Açores MoMAR observatory.
877 Deep Sea Res. Part Oceanogr. Res. Pap. 90, 62–75. https://doi.org/10.1016/j.dsr.2014.04.004

878 Sarrazin, J., Levesque, C., Juniper, S., Tivey, M., 2002. Mosaic community dynamics on Juan de Fuca
879 Ridge sulphide edifices: substratum, temperature and implications for trophic structure. CBM - Cahiers
880 de Biologie Marine 43, 275–279.

881 Sarrazin, J., Juniper, S.K., Massoth, G., Legendre, P., 1999. Physical and chemical factors influencing
882 species distributions on hydrothermal sulfide edifices of the Juan de Fuca Ridge, northeast Pacific. Mar.
883 Ecol. Prog. Ser. 190, 89–112. https://doi.org/10.3354/meps190089

884 Sarrazin, J., Legendre, P., de Busserolles, F., Fabri, M.-C., Guilini, K., Ivanenko, V.N., Morineaux, M.,
885 Vanreusel, A., Sarradin, P.-M., 2015a. Biodiversity patterns, environmental drivers and indicator
886 species on a high-temperature hydrothermal edifice, Mid-Atlantic Ridge. Deep Sea Res. Part II Top.

887 Stud. Oceanogr., Exploring New Frontiers in Deep-Sea Research: In Honor and Memory of Peter A.
888 Rona 121, 177–192. https://doi.org/10.1016/j.dsr2.2015.04.013

889 Sarrazin, J., Portail, M., Legrand, E., Cathalot, C., Laes, A., Lahaye, N., Sarradin, P.M., Husson, B., 2020.
890 Endogenous versus exogenous factors: What matters for vent mussel communities? Deep Sea Res.
891 Part Oceanogr. Res. Pap. 103260. https://doi.org/10.1016/j.dsr.2020.103260

892 Sarrazin, J., V, R., Sk, J., Jr, D., 1997. Biological and geological dynamics over four years on a high-
893 temperature sulfide structure at the Juan de Fuca Ridge hydrothermal observatory. Mar. Ecol. Prog.
894 Ser. 153, 5–24. https://doi.org/10.3354/meps153005

895 Scheirer, D.S., Shank, T.M., Fornari, D.J., 2006. Temperature variations at diffuse and focused flow
896 hydrothermal vent sites along the northern East Pacific Rise. Geochem. Geophys. Geosystems 7.
897 https://doi.org/10.1029/2005GC001094

898 Sen, A., Becker, E.L., Podowski, E.L., Wickes, L.N., Ma, S., Mullaugh, K.M., Hourdez, S., Luther, G.W.,
899 Fisher, C.R., 2013. Distribution of mega fauna on sulfide edifices on the Eastern Lau Spreading Center
900 and Valu Fa Ridge. Deep Sea Res. Part Oceanogr. Res. 72, 48–60.
901 https://doi.org/10.1016/j.dsr.2012.11.003

902 Sen, A., Podowski, E.L., Becker, E.L., Shearer, E.A., Gartman, A., Yücel, M., Hourdez, S., Luther, G.W., III,
903 Fisher, C.R., 2014. Community succession in hydrothermal vent habitats of the Eastern Lau Spreading
904 Center and Valu Fa Ridge, Tonga. Limnol. Oceanogr. 59, 1510–1528.
905 https://doi.org/10.4319/lo.2014.59.5.1510

906 Shank, T.M., Fornari, D.J., Von Damm, K.L., Lilley, M.D., Haymon, R.M., Lutz, R.A., 1998. Temporal and
907 spatial patterns of biological community development at nascent deep-sea hydrothermal vents
908 (9°50'N, East Pacific Rise). Deep Sea Res. Part II Top. Stud. Oceanogr. 45, 465–515.
909 https://doi.org/10.1016/S0967-0645(97)00089-1

910 Sousa, W.P., 1985. Disturbance and patch dynamics on rocky intertidal shores. The ecology of natural
911 disturbance and patch dynamics.

912 Spiess, F.N., Macdonald, K.C., Atwater, T., Ballard, R., Carranza, A., Cordoba, D., Cox, C., Garcia, V.M.,
913 Francheteau, J., Guerrero, J., Hawkins, J., Haymon, R., Hessler, R., Juteau, T., Kastner, M., Larson, R.,
914 Luyendyk, B., Macdougall, J.D., Miller, S., Normark, W., Orcutt, J., Rangin, C., 1980. East pacific rise: hot
915 springs and geophysical experiments. Science 207, 1421–1433.
916 https://doi.org/10.1126/science.207.4438.1421

917 Suzuki, K., Yoshida, K., Watanabe, H., Yamamoto, H., 2018. Mapping the resilience of chemosynthetic
918 communities in hydrothermal vent fields. Sci. Rep. 8, 9364. https://doi.org/10.1038/s41598-018-
919 27596-7

920 Tengberg, A., Hovdenes, J., Andersson, H.J., Brocandel, O., Diaz, R., Hebert, D., Arnerich, T., Huber, C.,
921 Körtzinger, A., Khripounoff, A., Rey, F., Rönning, C., Schimanski, J., Sommer, S., Stangelmayer, A., 2006.
922 Evaluation of a lifetime-based optode to measure oxygen in aquatic systems. Limnology and
923 Oceanography: Methods 4, 7–17. https://doi.org/10.4319/lom.2006.4.7

924 Tolstoy, M., Cowen, J.P., Baker, E.T., Fornari, D.J., Rubin, K.H., Shank, T.M., Waldhauser, F.,
925 Bohnenstiehl, D.R., Forsyth, D.W., Holmes, R.C., Love, B., Perfit, M.R., Weekly, R.T., Soule, S.A., Glazer,
926 B., 2006. A Sea-Floor Spreading Event Captured by Seismometers. Science 314, 1920–1922.
927 https://doi.org/10.1126/science.1133950

928   Tunnicliffe, V., 1991. The biology of hydrothermal vents : ecology and evolution. Biol. Hydrothermal
929   Vents Ecol. Evol. 29, 319–407.

930   Tunnicliffe, V., Embley, R.W., Holden, J.F., Butterfield, D.A., Massoth, G.J., Juniper, S.K., 1997. Biological
931   colonization of new hydrothermal vents following an eruption on Juan de Fuca Ridge. Deep Sea Res.
932   Part Oceanogr. Res. Pap. 44, 1627–1644. https://doi.org/10.1016/S0967-0637(97)00041-1

933   Van Audenhaege, L., Fariñas-Bermejo, A., Schultz, T., Lee Van Dover, C., 2019. An environmental
934   baseline for food webs at deep-sea hydrothermal vents in Manus Basin (Papua New Guinea). Deep Sea
935   Res. Part Oceanogr. Res. Pap. 148, 88–99. https://doi.org/10.1016/j.dsr.2019.04.018

936   Van Dover, C.L., 2007. The biological environment of polymetallic sulphides deposits, the potential
937   impact of exploration and mining on this environment, and data required to establish environmental
938   baselines in exploration areas. In: Polymetallic Sulphides and Cobalt-rich Ferromanganese Crusts
939   Deposits: Establishment of Environmental Baselines and an Associated Monitoring Programme during
940   Exploration. Proceedings of the International Seabed Authority's Workshop held in Kingston, Jamaica,
941   6e10 September 2004. Prepared by Offices of Resources and Environmental Monitoring (OREM), pp.
942   169e190. International Seabed Authority, Kingston, Jamaica: http://www.isa.org.jm/files/
943   documents/EN/Workshops/2004/Proceedings-ae.pdf. (accessed 13.06.13.).

944   Van Dover, C.L., 2011. Mining seafloor massive sulphides and biodiversity: what is at risk? ICES J. Mar.
945   Sci. 68, 341–348. https://doi.org/10.1093/icesjms/fsq086

946   Van Dover, C.L., 2010. Mining seafloor massive sulphides and biodiversity: what is at risk? ICES J. Mar.
947   Sci. 68, 341–348. https://doi.org/10.1093/icesjms/fsq086

948   Vuillemin, R., Le Roux, D., Dorval, P., Bucas, K., Sudreau, J.P., Hamon, M., Le Gall, C., Sarradin, P.M.,
949   2009. CHEMINI: A new in situ CHEmical MINIaturized analyzer. Deep Sea Res. Part Oceanogr. Res. Pap.
950   56, 1391–1399. https://doi.org/10.1016/j.dsr.2009.02.002

951   Washburn, T.W., Turner, P.J., Durden, J.M., Jones, D.O.B., Weaver, P., Van Dover, C.L., 2019. Ecological
952   risk   assessment   for   deep-sea   mining.   Ocean   Coast.   Manag.   176,   24–39.
953   https://doi.org/10.1016/j.ocecoaman.2019.04.014

954   Zajac, R.N., Whitlatch, R.B., Thrush, S.F., 1998. Recolonization and succession in soft-sediment infaunal
955   communities: the   spatial   scale   of   controlling   factors.   Hydrobiologia   375,   227–240.
956   https://doi.org/10.1023/A:1017032200173
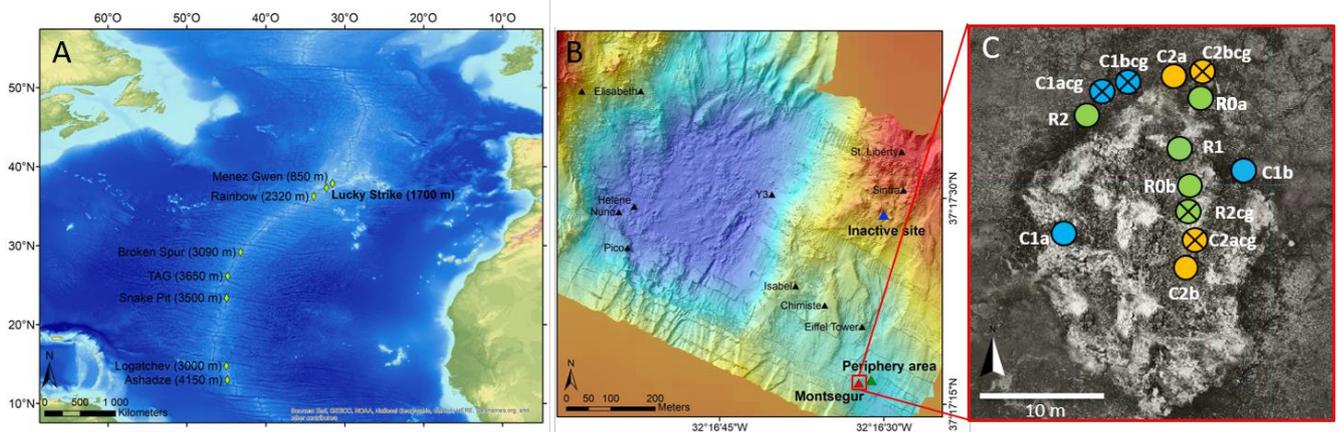
Figure 1. A. Location of the Lucky Strike (LS) vent field along the Mid-Atlantic Ridge. **B**. Bathymetric chart of LS and location of the Montségur edifice **C**. Position of the experimental and reference quadrats on and around the Montségur edifice. Green circles represent the reference quadrats, blue circles represent the experimental quadrats used to study the recolonisation 1 year after the disturbance, and orange circles represent the experimental quadrats used to study the recolonisation 2 years after the disturbance. Crossed off circles represent "caged" quadrats while empty circles represent quadrats without a cage.
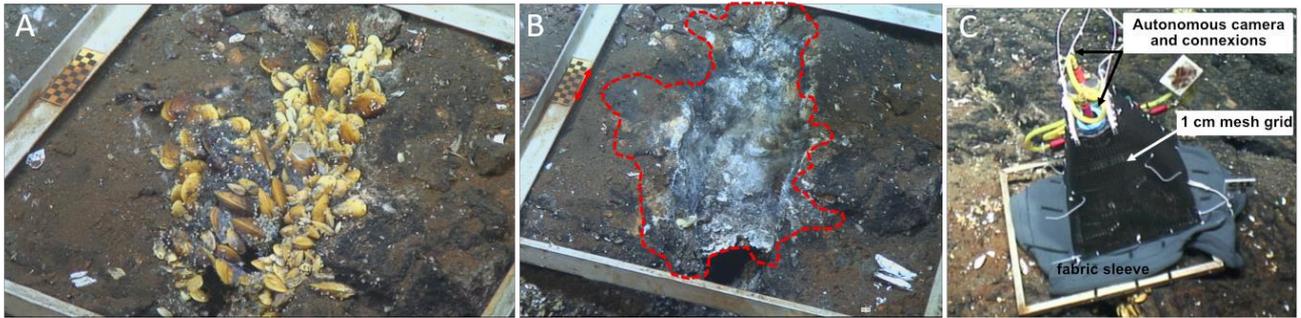
Figure 2. The C1a-cg experimental quadrat in 2017, (**A**) before faunal clearance (baseline community) and ; (**B**) after the induced disturbance. Red arrow highlights the check-board used to calibrate imagery analysis and estimate the sampling surface area (red dotted line). (**C**) The C1bcg "caged" experimental quadrat used to exclude large mobile predators. A 1 cm mesh grid was adjusted on the pyramidal structure on top of the quadrat (in black on the picture) and a grey fabric sleeve was attached to the edge of the caged quadrat to avoid colonisation of crawlers. A camera was deployed at the top of the pyramidal structure and connected to a battery on the side (yellow cables).
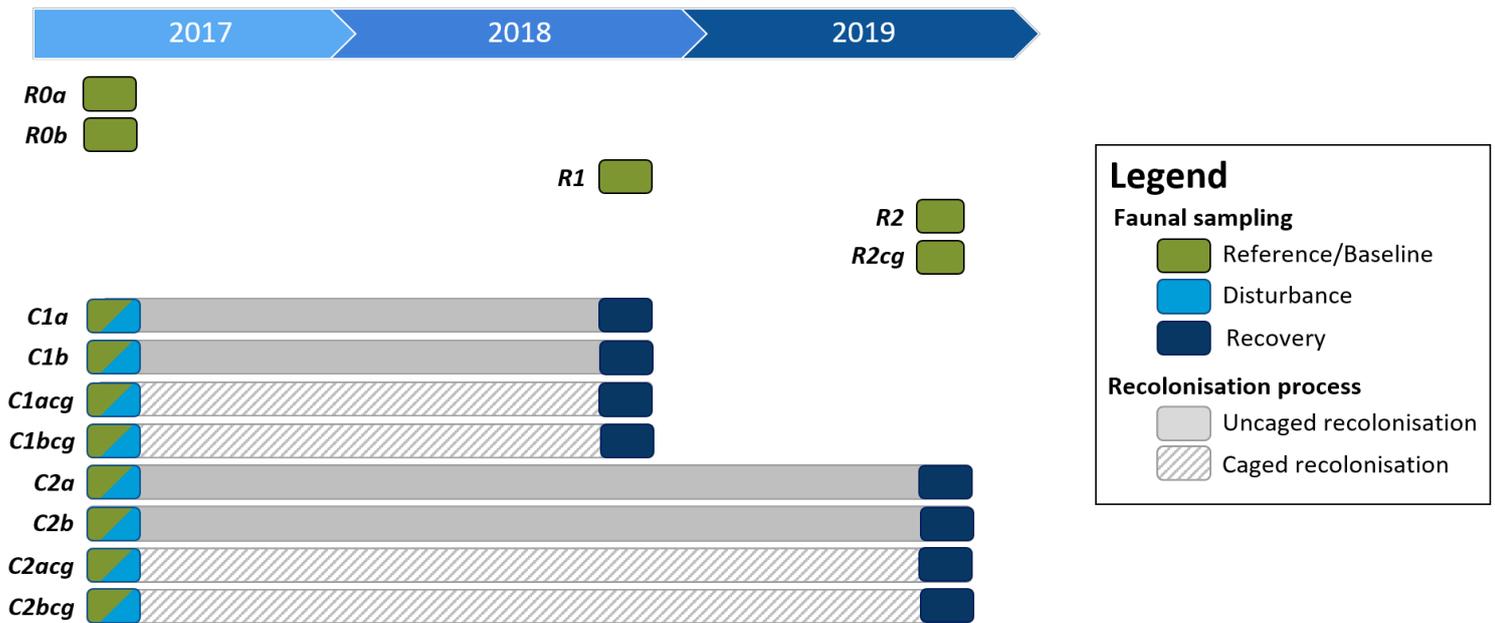
Figure 3. Experimental design of the disturbance experiment deployed between 2017 and 2019 on the Montségur edifice, Lucky Strike vent field (Mid-Atlantic Ridge). Small rectangles represent faunal sampling and their color indicates the nature of the operation: green, sampling of baseline communities; light blue, induction of disturbance by clearing faunal assemblages; dark blue, sampling after recolonisation to evaluate the recovery. Grey segments represent the recolonisation period studied for each quadrat. Hatched segments indicate the presence of caged during the recolonisation period.
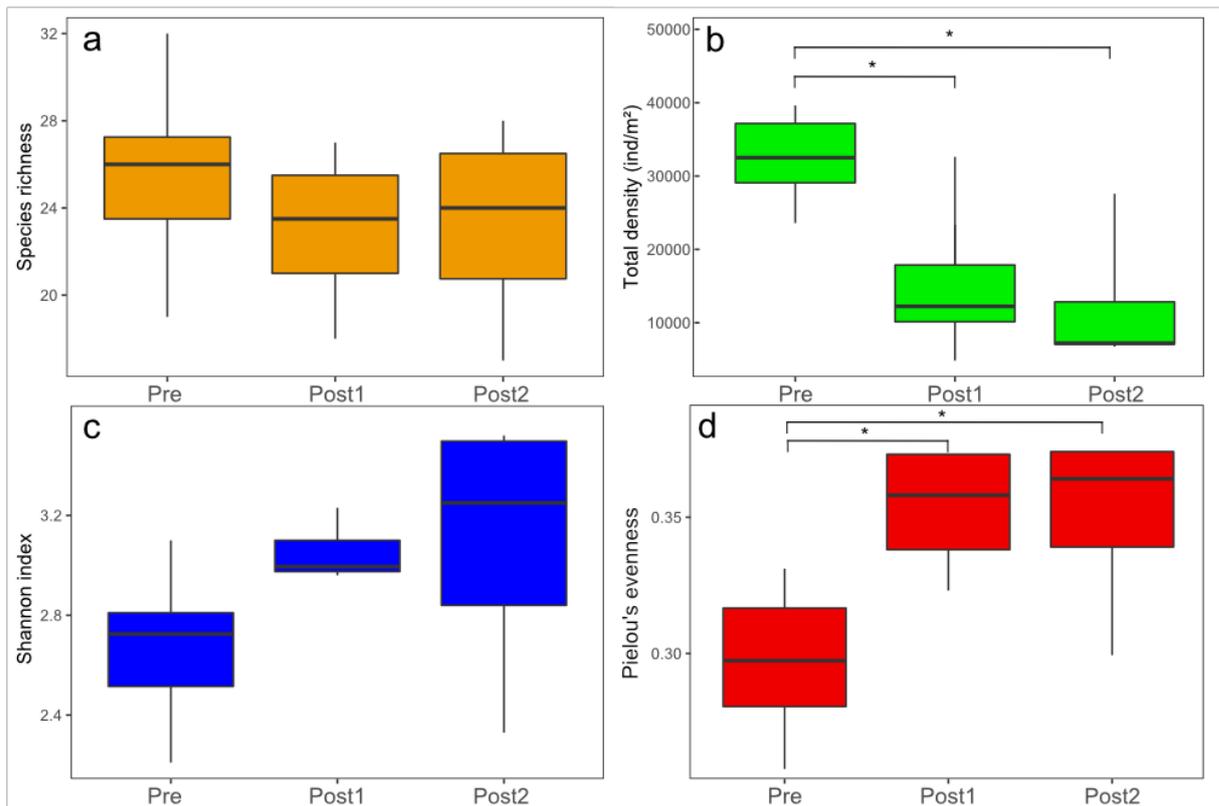
Figure 4. Species richness (**a**), total density (**b**), Shannon index (**c**) and Pielou's evenness index (**d**) of macrofaunal communities on the baseline communities and during the recolonisation process on the active Montségur edifice. Pre: assemblages sampled before the disturbance; Post1: assemblages sampled 1 year after the disturbance; Post2: assemblages sampled 2 years after the disturbance. Significance of Kruskall-Wallis multisample tests and post-hoc Dunn's tests are represented on the top of the boxplots.
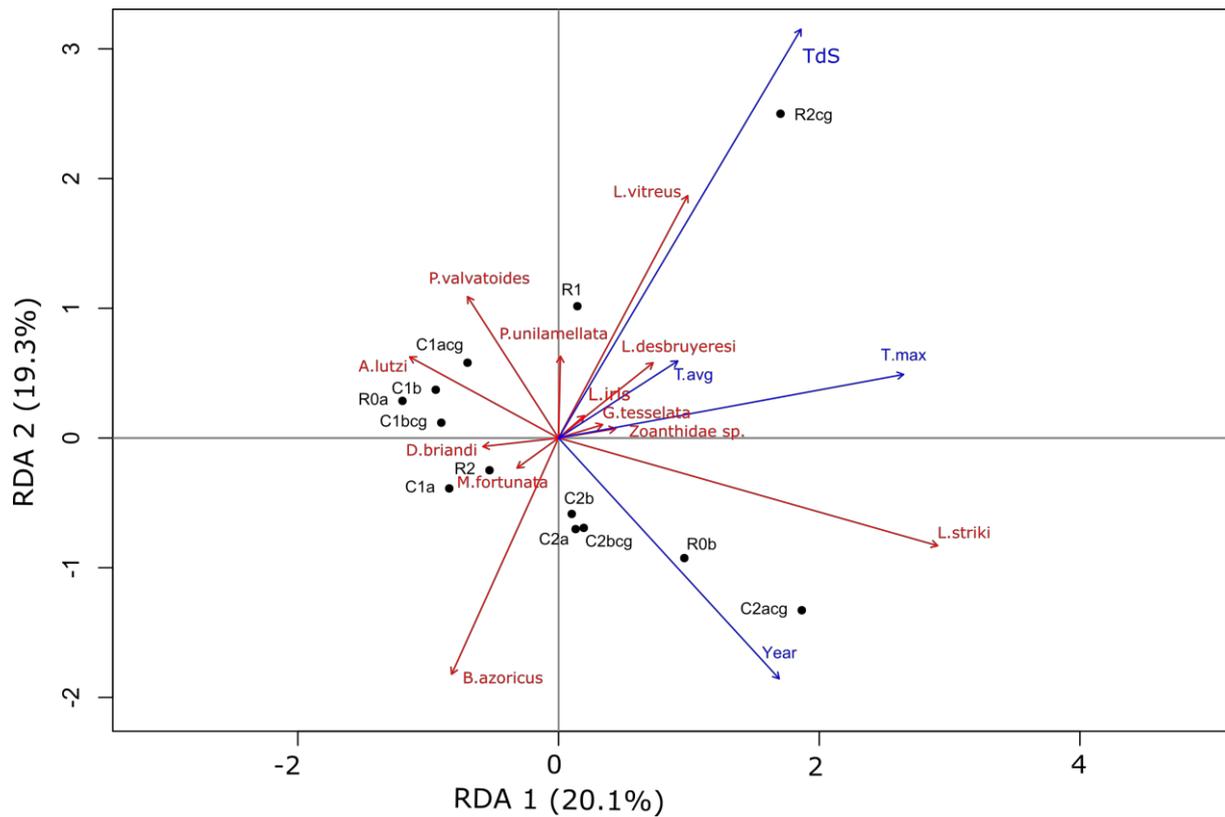
Figure 5. Canonical redundancy analysis (RDA, scaling 2) of Hellinger-transformed macrofaunal densities observed in the baseline community of the Montségur active edifice at the Lucky Strike vent field (Mid-Atlantic Ridge). The first canonical axis represents 20.1 % of the total variance in macrofaunal densities while the second axis represents 19.3% (adj R^2 = 25.1%, p = 0.004). The first axis is significant (p = 0.05). Only species that accounted for more than 50% of cumulative inertia on the two first axes are represented.
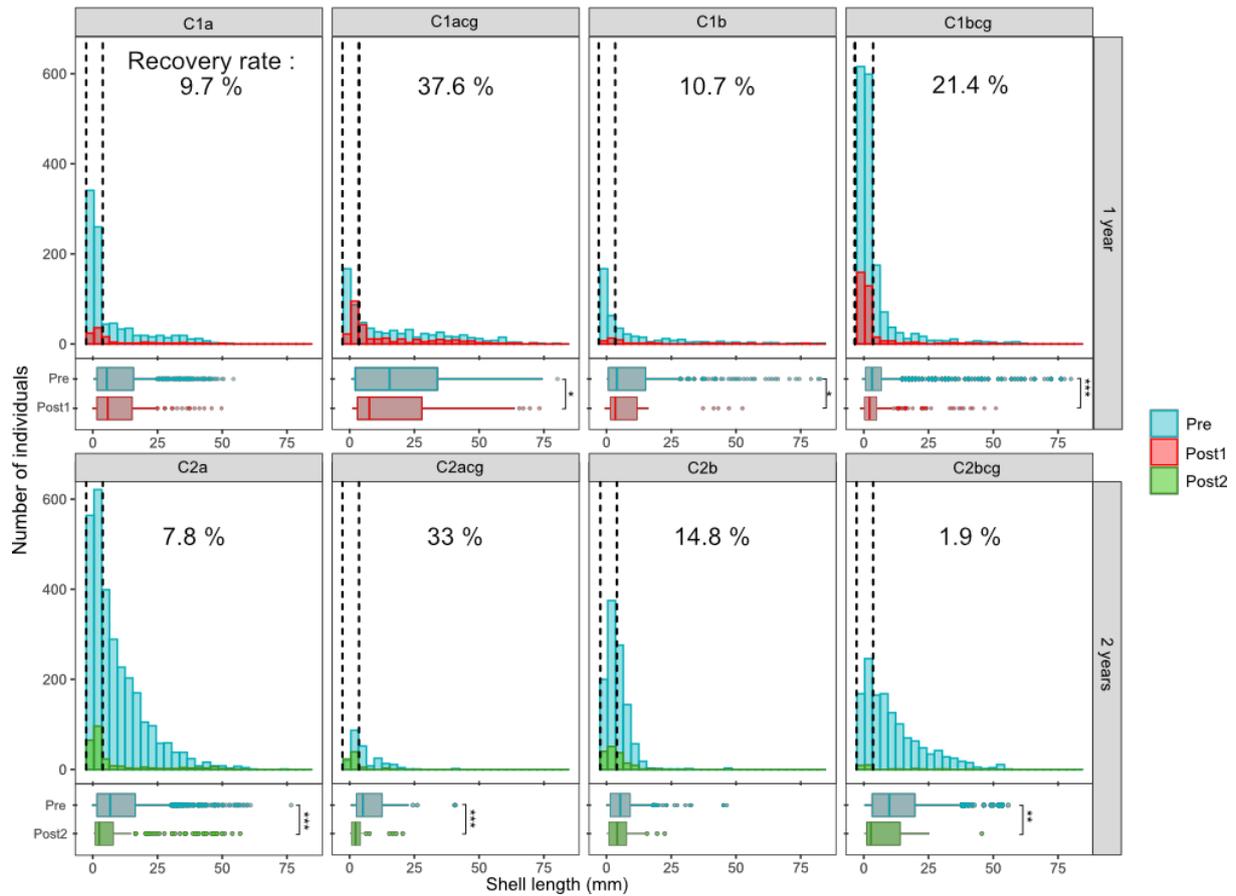
Figure 6. Histograms and boxplots of size frequency distribution of *Bathymodiolus azoricus* for each quadrat sampled at the Montségur edifice at the Lucky Strike vent field (Mid-Atlantic Ridge) including the pre-disturbed community (blue) and the communities one (red) and 2 (green) years after disturbance. Wilcoxon-Mann-Whitney tests were performed to identify differences in mean individual size between the baseline and post-disturbance communities. Asterisks indicate significant differences in mean shell length (*p-value<0.05; ** p-value <0.01; *** p-value <0.001). The interval between dotted lines represents the range of size at recruitment. The percentages represent the proportion of *B. azoricus* density which recovered in comparison of the pre-disturbed value in each quadrat.
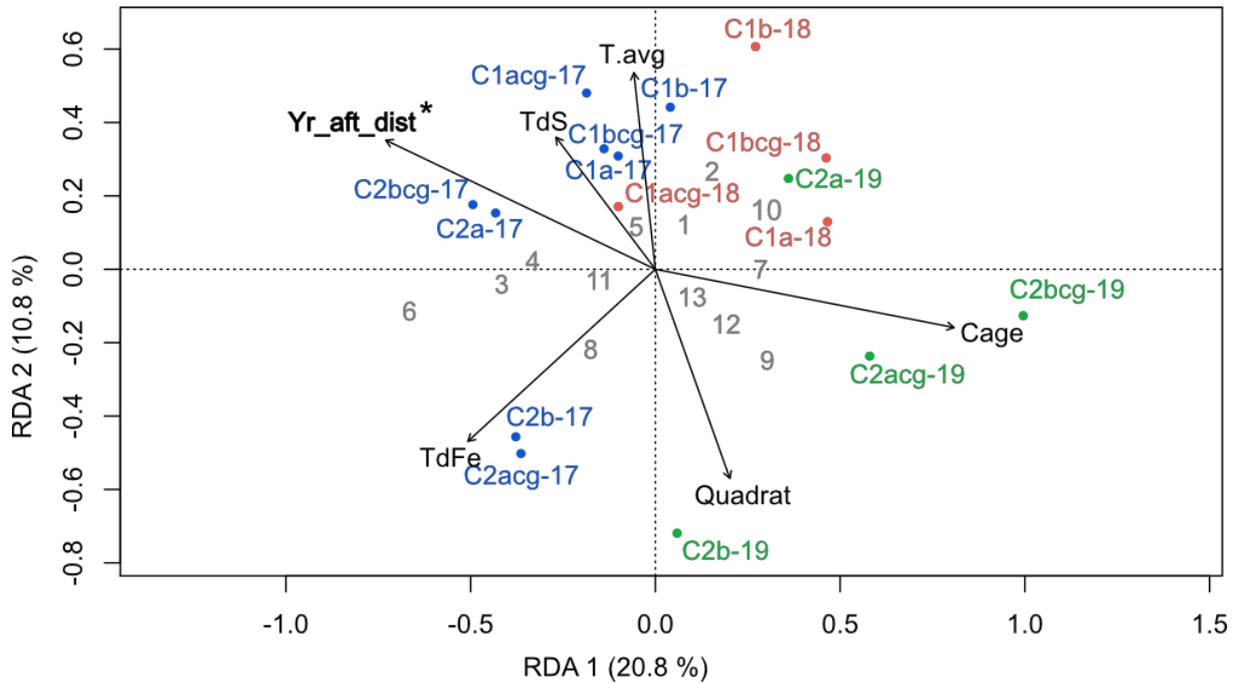
Figure 7. Canonical redundancy analysis (RDA, scaling 2) of Hellinger-transformed macrofaunal densities observed in the different assemblages during the recolonization process at the Montségur active edifice (Lucky Strike vent field, Mid-Atlantic Ridge). The first canonical axis represents 20.8% of the total variance in macrofaunal densities while the second axis represents 10.8% (with an adjusted R^2 of 20.5%). The RDA and the first axis are significant (p-values =0.006 and 0.023, respectively). Only species showing good fit with the first two canonical axes are represented. Colors refer to the time after disturbance: baseline communities (blue); 1 year after disturbance (red); two years after disturbance (green). Explanatory variables: Years after disturbance (*Yr_aft_dist*), average temperature measured before sampling (*T.avg*), mean concentration of total dissolved sulphides (*TdS*), mean concentration of total dissolved iron (*TdFe*), if quadrats are caged or uncaged (*Cage*), identification of quadrats to test the dependence of the same location over the time of the experiment (*Quadrat*). Response variables, each species is designated by a number: 1 – *Amphisamytha lutzi*; 2 – *Aphotopontius sp.*; 3 – *Bathymodiolus azoricus*; 4 – *Branchipolynoe seepensis*; 5 – *Lepetodrilus atlanticus*; 6 – *Lirapex costellata*; 7 – *Laeviphitus desbruyeresi*; 8 – *Luckia striki*; 9 – *Lurifax vitreus*; 10 – *Oncholaimus dyvae*; 11 – *Paralepetopsis ferrugivora*; 12 – *Protolira valvatoides*; 13 – *Xylodiscula analoga*.
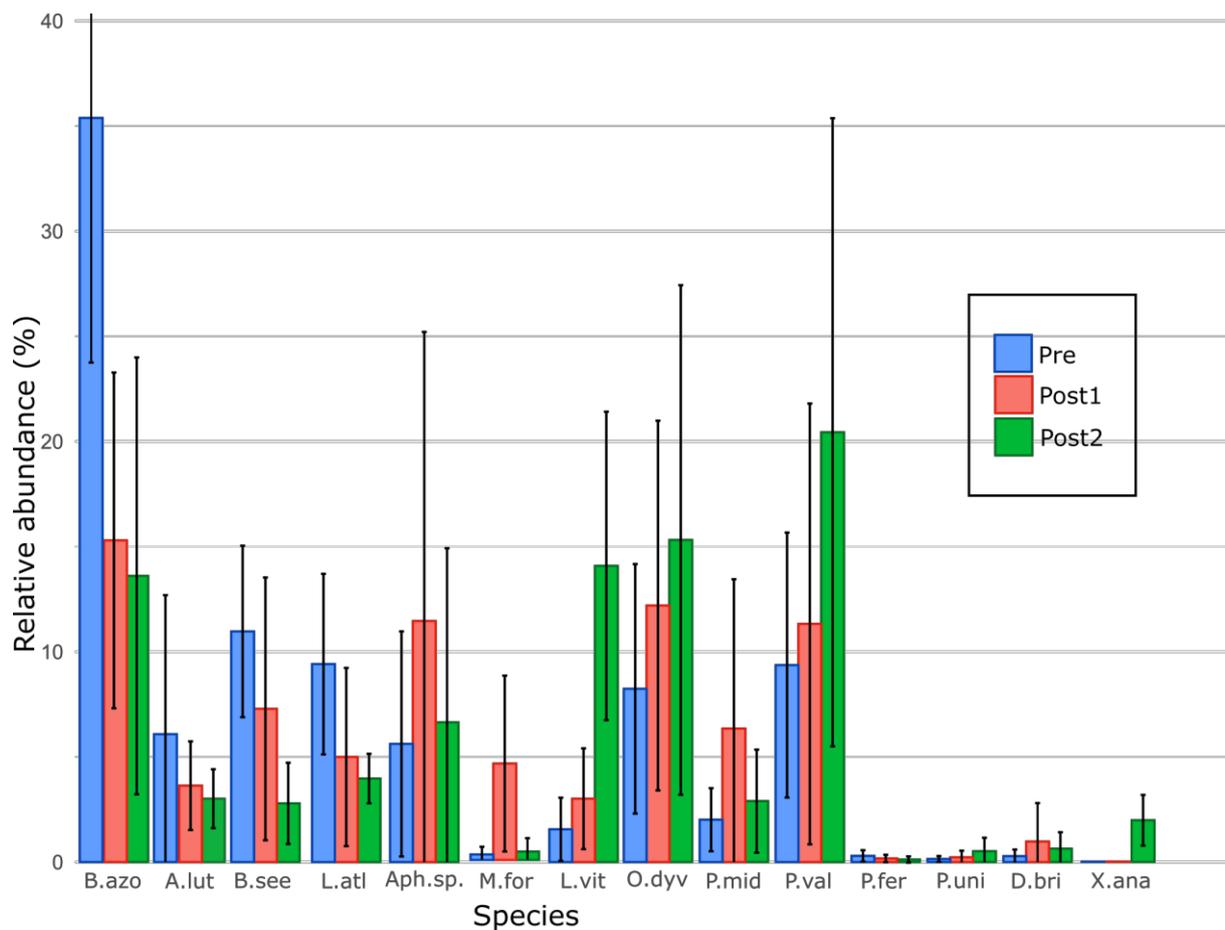
Figure 8. Mean and standard deviations of densities for the most abundant species among the experimental quadrats on the active Montségur edifice before the disturbance (Pre) and one/two years after the disturbance (Post1 and Post2). Species acronyms: B.azo – *Bathymodiolus azoricus*, A.lut – *Amphisamytha lutzi*; B.see – *Branchipolynoe seepensis*; L.atl – *Lepetodrilus atlanticus*; Aph.sp. – *Aphotopontius sp.*; M.for – *Mirocaris fortunata*; L.vit – *Lurifax vitreus*; O.dyv – *Oncholaimus dyvae*; P.mid – *Pseudorimula midatlantica*; P.val – *Protolira valvatoides*; P.uni – *Prionospio unilamellata*; D.bri – *Divia briandi*; X.ana – *Xylodiscula analoga*.
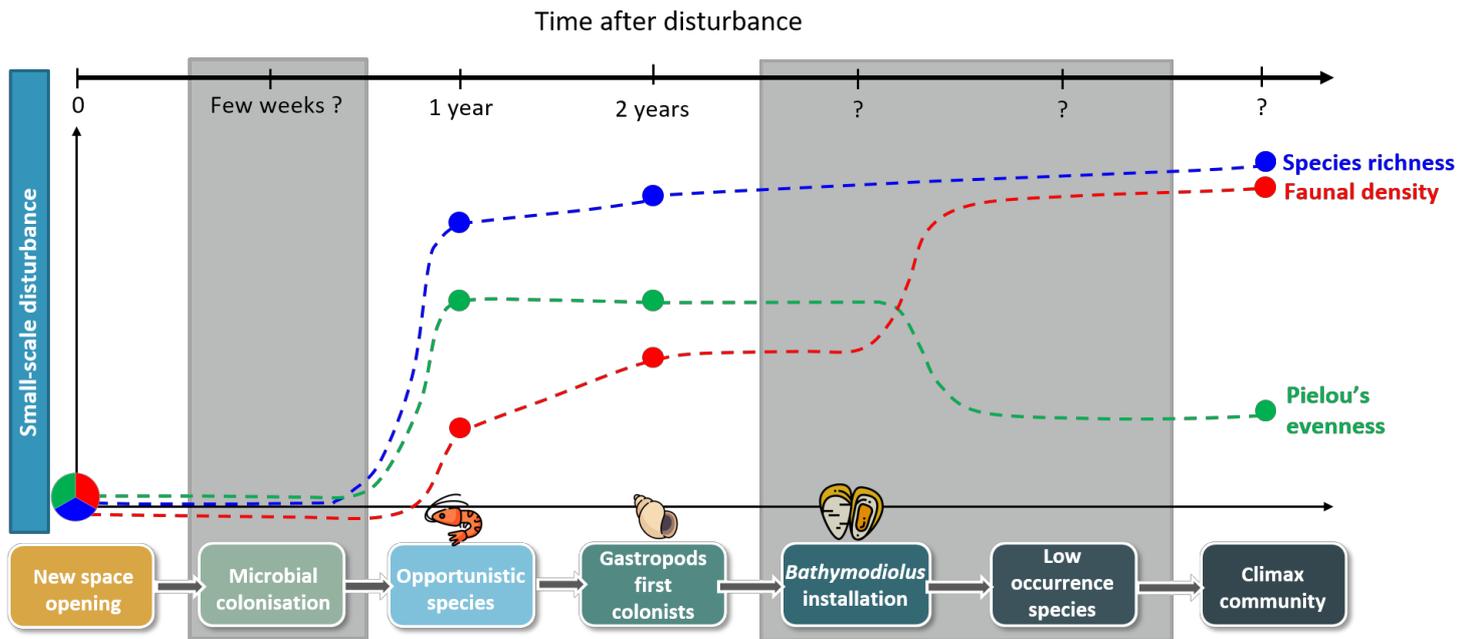
Figure 9. Conceptual model of colonisation and ecological succession until climax after a small-scale disturbance on the Lucky Strike vent assemblages (MAR). Evolution of species richness, faunal densities and Pielou's evenness index during the recovery process, based on the main results of our disturbance experiment (solid dots) and inferred from the literature (grey boxes).

Table 1. Environmental conditions on the baseline communities of the different quadrats deployed on the Montségur edifice (Lucky Strike vent field, Mid-Atlantic Ridge). Temperature: average: T.avg., standard deviation: T.std. maximum: T.max and minimum: T.min. from iButtons[TM]. Oxygen (O_2). Total dissolved sulphide (TdS) and Total dissolved iron (TdFe) measured with the *in situ* analysers CHEMINI. Methane (CH_4) and pH were measured through quantitative analyses from samples collected with the PEPITO water sampler (Sarradin et al. 2009). Highest values are highlighted in bold and lowest values in grey.

Quadrat	T.avg	T.std	T.min	T.max	O_2 (µM)	TdS (µM)	TdFe (µM)	CH_4 (µM)	pH
					Mean ± SD				
Montségur									
R0a	*5.2*	*0.2*	4.6	*6.1*	*208.2 ± 0.1*	2.7 ± 0.2	0.2 ± 0.1	0.4	**7.8**
R0b	6.9	0.8	5.1	11.5	207.2 ± 0.4	3.1 ± 1.0	1.1 ± 0.3	0.5	7.6
R1	**9.5**	**2.7**	**6.1**	**22.1**	206.1 ± 1.1	2.3 ± 0.2	**2.2 ± 0.2**	**2.1**	7.2
R2	5.5	0.4	5.1	11.4	206.9 ± 1.3	3.2 ± 2.7	0.2 ± 0.1	0.9	7.5
R2cg	5.3	0.2	4.6	7.1	205.6 ± 0.6	0.9 ± 0.2	0.6 ± 1.1	*0.2*	7.9
C1a	6.1	0.3	5.1	7.1	207.4 ± 0.1	3.2 ± 0.8	0.2 ± 0.1	0.7	7.6
C1acg	5.8	1.2	4.6	12.1	204.3 ± 1.5	3.9 ± 2.6	0.3 ± 0.1	**2.1**	7.2
C1b	6.4	0.4	4.6	10.6	206.2 ± 1	**10.8 ± 14.7**	0.3 ± 0.3	1.1	7.4
C1bcg	5.7	0.42	4.6	8.1	207.9 ± 0.4	2.5 ± 0.6	0.2 ± 0.1	0.8	7.7
C2a	**7.6**	**1.12**	**6.1**	**16.1**	203.8 ± 2.1	**23.2 ± 26.3**	1.1 ± 0.3	**15.2**	6.1
C2acg	6.3	0.5	5	8.6	207.4 ± 0.8	1.3 ± 0.1	0.9 ± 0.8	0.7	7.7
C2b	5.3	0.2	5	*6.1*	205.2 ± 0.5	3.8 ± 3.8	0.9 ± 0.4	0.4	7.8
C2bcg	5.3	0.3	4.6	6.6	206.6 ± 0.3	5.6 ± 1.2	0.2 ± 0.1	**2.0**	7.2

Do not remove this file (contains research data)

Click here to access/download
RDM Data Profile XML
DataProfile_5815735.xml

Declaration of interest

The authors declare no competing interests.

Author Statement

JM, MM and JS conceived the ideas and designed the methodology. JM, MM, JS, ALH and CC collected the samples on board during oceanographic cruises. JM, MM, JS, ALH, CC, JPD and SH processed and analysed the data. JM and RL did the statistical analyses. JM, MM, ERL and JS discussed and interpreted the results. JM wrote the first draft of the manuscript and all authors commented on previous versions of the manuscript. All authors read and approved the final manuscript.